

Artificial Molecular Ratchets: Tools Enabling Endergonic Processes

Thitiporn Sangchai⁺, Shaymaa Al Shehimi⁺, Emanuele Penocchio,^{*} and Giulio Ragazzon^{*}



Abstract: Non-equilibrium chemical systems underpin multiple domains of contemporary interest, including supramolecular chemistry, molecular machines, systems chemistry, prebiotic chemistry, and energy transduction. Experimental chemists are now pioneering the realization of artificial systems that can harvest energy away from equilibrium. In this tutorial Review, we provide an overview of artificial molecular ratchets: the chemical mechanisms enabling energy absorption from the environment. By focusing on the mechanism type—rather than the application domain or energy source—we offer a unifying picture of seemingly disparate phenomena, which we hope will foster progress in this fascinating domain of science.

1. Introduction

Bulk endergonic processes—having $\Delta G > 0$ —are thermodynamically impossible without an energy source. Yet, they are essential in many chemical processes, including life. There, they underlie structure formation, energy transduction, and the operation of molecular machinery.^[1] Moreover, if we consider the new classes of problems identified by Whitesides to reinvent modern chemistry,^[2] almost half of them are related to the ability of chemists to unravel and engineer endergonic reactions. Two examples are understanding how the brain thinks and developing adaptive materials. An energy input alone is not sufficient to make an endergonic reaction occur. There needs to be a mechanism that enables transferring some of the input energy to the target endergonic process: a ratchet mechanism.^[3–8]

Historically, the development of artificial molecular ratchet mechanisms has been tightly associated with the emergence of directionality in space, e.g., to mimic processive motor proteins or adenosine triphosphate (ATP) synthase rotary motor. However, spatial directionality appears as an additional layer of complexity, which is conditional to the rectification of chemical reactions (i.e., having directed fluxes in a chemical reaction network). Thus, the rectification of chemical reactions appears as a more fundamental aspect: it is a necessary prerequisite for directionality in space—yet not sufficient. Moreover, the rectification of chemical currents can be precisely described, whereas directionality in space is a very intuitive concept at first sight, but it is very difficult to draw a precise boundary associated with its occurrence.

All ratchet mechanisms rectify chemical reactions by coupling two distinct reactions: a driving one—which provides energy by proceeding towards equilibrium—and a driven one—which absorbs part of the energy to proceed against the thermodynamic potential. These two reactions must be part of the same reaction network. Let's consider a minimal system, where the driven reaction is the interconversion of a low-energy state L to a high-energy state H. For the driving reaction to transfer part of its energy to the $L \rightleftharpoons H$ interconversion, there needs to be another path—involving the driving reaction—leading from L to H, forming a chemical reaction cycle (Figure 1a). Ratcheting is associated with the directional occurrence of such a chemical reaction cycle. In particular, a ratchet mechanism can be present when it is possible to identify a sequence of steps in the network that result in the simultaneous occurrence of both the driving and the driven reaction (see below). Therefore, in the following we will indicate explicitly in the Figures which reactions have this role.

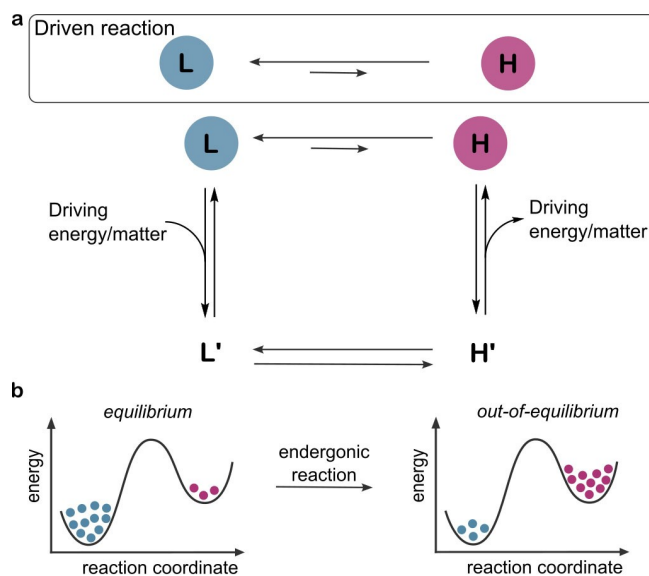


Figure 1. a) Target reaction to be driven away from equilibrium, by converting a low-energy state L into a high-energy state H, and cyclic reaction network associated with the conversion of L into H enabled by the consumption of energy. Vertical arrows indicate generic processes exchanging energy and/or matter with the system. b) Representation of an endergonic reaction shifting the equilibrium distribution of L and H towards H. Shifting the equilibrium distribution towards L would also be an endergonic process (not represented).

[*] T. Sangchai,[†] Dr. S. Al Shehimi,[†] Dr. G. Ragazzon
University of Strasbourg, CNRS, Institut de Science et d'Ingénierie
Supramoléculaires (ISIS) UMR 7006
8 allée Gaspard Monge, 67000 Strasbourg (France)
E-mail: ragazzon@unistra.fr

Dr. E. Penocchio
Department of Chemistry, Northwestern University
2145 Sheridan Road, Evanston, IL 60208 (USA)
E-mail: emanuele.penocchio@northwestern.edu

[†] These authors contributed equally to this work.

© 2023 The Authors. Angewandte Chemie International Edition published by Wiley-VCH GmbH. This is an open access article under the terms of the Creative Commons Attribution Non-Commercial License, which permits use, distribution and reproduction in any medium, provided the original work is properly cited and is not used for commercial purposes.

Regardless of the energy source, there are two main ratchet mechanisms: energy and information ratchets. The term “energy ratchet” comes from the fact that the *energy* of the intermediates of the cycle is important in dictating the directionality of the network. In most cases, energy ratchets require an energy supply that changes over time or in space, e.g., the sequential addition of an acid and a base, or a reductant and an oxidant. On the contrary, information ratchets do not depend on the energy of intermediates, which are irrelevant in determining the directionality in the network. In these systems, the rate of the energy-providing reaction depends on the state of the reaction network from which the reaction takes place; i.e., which intermediates are involved. Therefore, the occurrence of the energy-providing reaction depends on the *information* of which intermediates of the chemical reaction network are populated, from which the term “information ratchet”.

In this tutorial review, we provide a compass to orient readers interested in this area. We present the basic operating principles of molecular ratchet mechanisms focusing on the rectification of chemical currents. For a description of ratchets in the context of directionality in space, we refer the readers to other excellent reviews on artificial molecular machines.^[7,9–11] In selecting the examples, we aimed at being didactic and representative, while we could not be comprehensive. We acknowledge that other equally valid choices might have been made, and we referred readers to comprehensive sectorial reviews in the dedicated sections.

To complete setting the context, we clarify that this manuscript focuses on fully synthetic systems operating in

solution as an ensemble and treats them using mass-action kinetics. We choose this framework among a few (e.g., stochastic systems, etc.),^[3,8,12–14] because it corresponds to the classical laboratory conditions employed to study synthetic molecules and only requires familiarity with basic chemical kinetics to be understood. As a result, our terminology refers to concentrations, rather than single molecular entities. For instance, when discussing the energetic properties of a given reaction, we consider how the concentration of species differs from their equilibrium values, quantified by the nonstandard free energy change (ΔG) of a given reaction, namely the difference between the chemical potential of the products and reactants (sometimes denoted as $\Delta_r G$ or $\Delta\mu$ in the literature). As a result, an endergonic reaction absorbs energy shifting the distribution of species away from equilibrium (Figure 1b). The opposite reaction is also a (non-equilibrium) process, but the system dissipates energy relaxing toward equilibrium, rather than moving away from it. The same conceptual framework was adopted for example by Branscomb et al., who discussed molecular ratchets as mechanisms that convert disequilibria, noting that this approach implies that energy is not stored in “high-energy” bonds, but rather in distributions.^[15]

The tutorial review is organized as follows. We first describe energy and information ratchet mechanisms, alternating literature examples with their principles, and touching on spatial phenomena. Then, we discuss cases in which these mechanisms can coexist, and proceed illustrating energetic features that characterize molecular ratchets



Thitiporn Sangchai is a Ph.D. student at Institut de Science et d'Ingénierie Supramoléculaires, University of Strasbourg. His B.Sc. was dedicated on catalytic asymmetric synthesis with internships at the University of Texas at Arlington and Mahidol University. After obtaining his B.Sc., he pursued his M.Sc. at the University of Rennes 1, conducting research on materials chemistry on pi-conjugated P-heterocycles for opto-electronic applications. In 2022, he broadened his research perspective, delving into the development of non-equilibrium chemical systems.



Shaymaa Al Shehimi holds a Bachelor's degree in Chemistry from the Lebanese University. She obtained her Master's degree in Catalysis Molecules and Green Chemistry from the University of Rennes 1. During her Ph.D. at ENS de Lyon, she conducted research at the interface of Supramolecular Chemistry and Physical Chemistry under the supervision of Dr. Bucher. She is currently a postdoctoral researcher in the group of Dr. Ragazzon at the Institut de Science et d'Ingénierie Supramoléculaires in Strasbourg, investigating minimal chemical ratchets.



Emanuele Penocchio is a postdoc in the Department of Chemistry at Northwestern University. After studying chemistry, he obtained a Ph.D. in Physics in 2022, with a thesis on the non-equilibrium thermodynamics of chemical reaction networks. Emanuele's research focuses on the physical chemistry underlying chemical systems that consume energy to perform functions. He believes in the dialogue between theoreticians and experimentalists as a way to identify worth-answering theoretical questions. More about Emanuele at <https://emanuelepenocchio.github.io/>.



Giulio Ragazzon is a junior group leader at the Institut de Science et d'Ingénierie Supramoléculaires (ISIS) of the University of Strasbourg. After obtaining his Ph.D. in 2017, with a thesis on molecular machines, he studied self-assembling systems and catalytic carbon-based materials. These experiences served as a basis to develop non-equilibrium chemical systems that perform endergonic processes by absorbing energy from the environment. You can get to know more about Giulio and his group at <https://ragazzonlab.isis.unistra.fr/>.

operation. Connections to other fields are also presented, before concluding with an outlook.

2. Energy Ratchets

2.1. Chemically-Driven Energy Ratchets

Energy ratchets are by far the most exploited ratchet mechanisms in synthetic systems. To illustrate their operation, we introduce the endergonic assembly of a pseudorotaxane driven by the alternation of redox stimuli.^[16] The system is composed of macrocycle $\mathbf{1}^{4+}$ and dumbbell $\mathbf{2}^{3+}$ (Figure 2), which comprise redox-active viologen moieties in their structure. Due to charge repulsion, the formation of corresponding pseudorotaxane $[\mathbf{2}^{3+} \subset \mathbf{1}^{4+}]$ is negligible at millimolar concentration in an organic solvent—the typical experimental conditions. Assembly of this pseudorotaxane is the endergonic reaction promoted by the ratchet mechanism. The reaction providing the energy necessary to make it happen is the redox reaction between metallic zinc (reductant) and tris(4-bromophenyl)ammonium cation (oxidant). These reagents are added in sequence, affording an alternation of environmental redox conditions. The addition of Zn^0 causes the reduction of viologen units, affording $\mathbf{1}^{2(+\bullet)}$ and $\mathbf{2}^{1(+\bullet)}$. These species are prone to self-assembly due to radical-radical interactions; as a result, reduction affords pseudorotaxane $[\mathbf{2}^{1(+\bullet)} \subset \mathbf{1}^{2(+\bullet)}]$, which is thermodynamically stable under reducing conditions. Addition of an oxidant restores the initial fully oxidized components; however, if the oxidation is faster than disassembly, the resulting state is mostly composed of pseudorotaxane $[\mathbf{2}^{3+} \subset \mathbf{1}^{4+}]$, which becomes present in

concentrations not compatible with its self-assembly equilibrium, completing an endergonic reaction. As for any non-equilibrium distribution, the system relaxes over time to equilibrium, here reverting to the separated components.

In this example, threading and dethreading reactions occur through the same end of dumbbell $\mathbf{2}$, the pyridinium one. There is a directionality in the chemical reaction network (counterclockwise chemical current in Figure 2), but the dumbbell does not transit through the macrocycle in a unidirectional way. Such a directionality in space was achieved by introducing a neutral isopropylphenyl pseudostopper in dumbbells analogous to $\mathbf{2}^{3+}$.^[17,18] In the oxidized state, the pyridinium terminal offers a barrier that is higher than the corresponding pseudostopper; the pyridinium barrier is instead lower once the macrocycle is reduced, due to a decreased electrostatic repulsion between the macrocycle and the pyridinium.^[19] As a result, threading in the reduced state occurs preferentially through the pyridinium end, while subsequent oxidation induces a relocation onto the collecting chain by shuttling of the macrocycle through the pseudostopper unit. This structure enables using repeated additions of redox agents to progressively drive the system away from equilibrium, for example by accumulating more macrocycles onto the dumbbell. This ability was first demonstrated by pumping two macrocycles onto the collecting chain and then further expanded to pump up to ten macrocycles, as well as in related structures and directional motors.^[20–22] With this discussion we want to highlight that imparting directionality in a chemical reaction network is already a non-equilibrium phenomenon enabled by a ratchet mechanism. To obtain a directionality in space and drive the system progressively away from

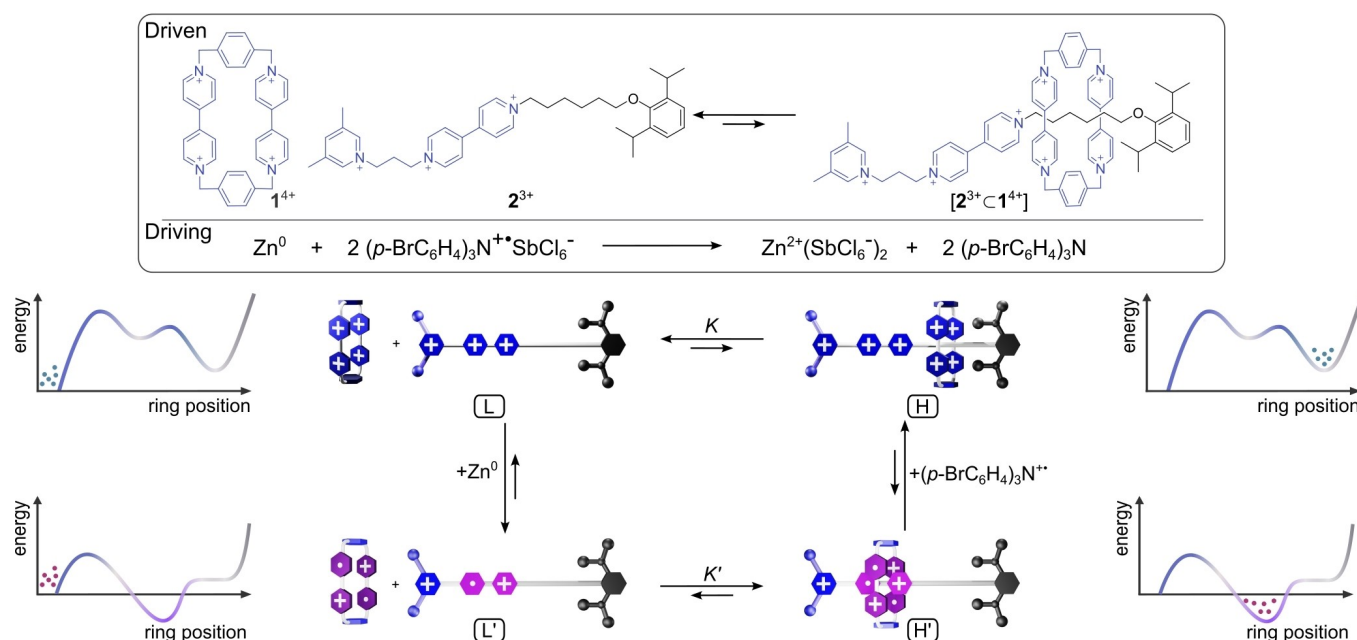


Figure 2. Chemical reaction network and potential energy surfaces associated with the formation of a high-energy pseudorotaxane, enabled by an energy ratchet mechanism powered by a redox reaction.

equilibrium, it seems necessary to satisfy additional requirements.

The concept of energy ratcheting is not limited to molecular machines. By combining two orthogonal reactions, it is possible to obtain square reaction schemes resembling the one just discussed. A possibility is to combine imine formation with the addition and removal of a templating metal ion (Figure 3).^[23] In this study, when a bis-aldehyde is mixed with a bis-amine, imine formation affords the thermodynamically stable [2+2] macrocycle **3₂**. Addition of Cd²⁺ templates the formation of the [1+1] macrocycle [Cd·**3**]²⁺. Then, removal of Cd²⁺ by adding complexing agent **4** affords the metal-free [1+1] macrocycle **3**, a high-energy species under the employed experimental conditions. Macrocycle **3** is strained and has an enhanced reactivity for imine hydrolysis with respect to the thermodynamic imine products. More recently, the same strategy has been employed by Prins and co-workers to assemble a dynamic covalent hydrazone.^[24] In this case, ATP served as templating agent, which was removed enzymatically. The resulting adduct had enhanced catalytic activity towards hydrolysis of a ribonucleic acid (RNA) model substrate. A feature shared by these systems is that the final state depends on the sequence of stimuli applied; as a result, energy ratchet mechanisms may offer guidance in sequence-dependent processes, such as sequence-dependent non-covalent synthesis.^[25]

2.2. Principles of Chemically-Driven Energy Ratchets

In the examples introduced so far, systems are exposed to different environments by adding chemicals sequentially.

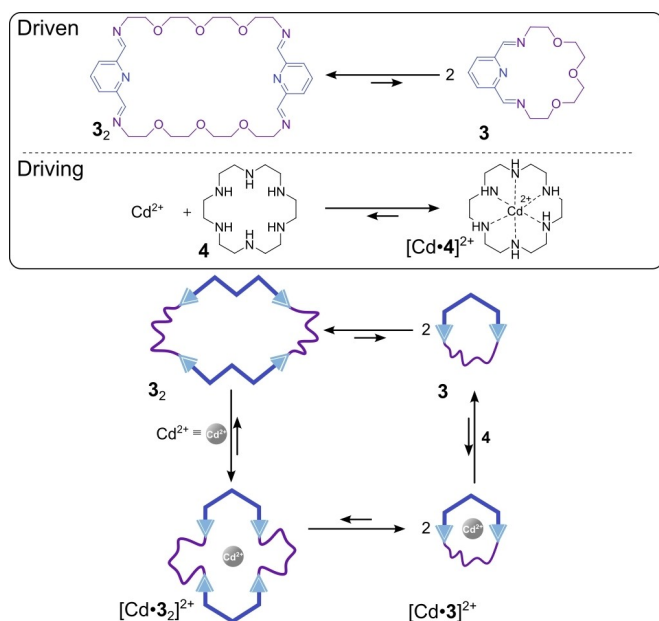


Figure 3. a) Reaction network associated with the rearrangement of a dynamic covalent library driven by metal coordination, according to an energy ratchet mechanism.

In practice, an operator makes an addition at a specific time, which makes the systems non-autonomous: the vertical arrows in Figure 2 represent processes that only happen at the specific time of addition, e.g., in case of alternating redox conditions, all the species are oxidized or reduced simultaneously. To describe the working principles, we use the reaction network in Figure 1, which can be used to map the square networks described in section 2.1, while being simpler as it includes only unimolecular steps. We can consider a starting situation in which only species L and H are present, and the reaction $L \rightleftharpoons H$ is at equilibrium, favoring L over H according to the equilibrium constant K . By suddenly changing the environment, assuming that these processes are instantaneous on the time scale of the horizontal chemical reactions and undergo full completion, all L and H species convert into L' and H', respectively. Then, the system will eventually relax to a new equilibrium dictated by the equilibrium constant K' of the reaction $L' \rightleftharpoons H'$. When the system's environment is switched back to the original condition, immediately after the switch the L and H species population will be distributed according to the equilibrium constant K' , namely $[H]/[L] = K'$. If $K' > K$, the effect of changing the system's environment back and forth would be to drive the system to a non-equilibrium distribution ($[H]/[L] > K$) through the induction of a chemical current from L to H through the path $L \rightarrow L' \rightarrow H' \rightarrow H$. Importantly, the overall reaction associated with this sequence of steps corresponds to the sum of the driving and driven reaction. The generation of concentration distributions that are not compatible with all the reactions in the system being at equilibrium (detailed balance) is a fully general outcome of a ratchet operation. As for any non-equilibrium system, if enough time is given, the non-equilibrium populations will ultimately revert to equilibrium.

The above example illustrates that an essential requirement for the operation of energy ratchet mechanisms is a difference in the equilibrium constants of the driven reaction in the two alternating environments ($K \neq K'$). Indeed, when the system's environment does not affect the horizontal equilibria, $K' = K$ and switching environment cannot affect species distribution. For instance, to achieve the endergonic assembly of pseudorotaxanes with the system in Figure 2, the self-assembly reactions must have different equilibrium constants in the oxidized and reduced states. Furthermore, the system's directionality is fully controlled by the ratio K'/K . Indeed, when $K' < K$, the ratchet mechanism favors the accumulation of L species with respect to the initial equilibrium via a right-to-left chemical current $H \rightarrow H' \rightarrow L' \rightarrow L$. Therefore, the relative stability—i.e., energy—of the involved states plays a crucial role in determining the outcome of energy consumption, highlighting why similar mechanisms fall under the category of “energy” ratchets. A corollary of this observation is that one way to recognize if an energy ratchet mechanism is active in a given system is to perform the thought experiment of inverting the stability of states involved and observing if the directionality is also inverted.^[15] For instance, in Figure 2, this hypothetical test would correspond

to favoring assembly in the oxidized state and disassembly in the reduced state. If an inversion in the accumulation of species is expected, it implies that the system is dominated by an energy ratchet mechanism.

Until now, we reasoned on what happens to the $[H]/[L]$ ratio right after the system's environment is switched back to the original condition upon a sequence of external manipulations. As anticipated, with time, species' concentrations will return to the equilibrium distribution dictated by K , cancelling the non-autonomous energy ratchet mechanism's effect. However, if H is a kinetically trapped species, the non-equilibrium distribution generated by the ratcheting cycle may be stable for a long time. This is indeed the case for the system in Figure 2, in which the dethreading of 1^{4+} is hampered by the electrostatic barrier constituted by the 3,5-dimethylpyridinium cation-terminating 2^{3+} . If none of the species is kinetically stable, the ratcheting cycle can be repeated periodically to sustain the non-equilibrium distribution. This periodic, non-autonomous driving process will lead to periodic variations of species concentrations, with a cyclic chemical current along the pathway $L \rightarrow L' \rightarrow H' \rightarrow H \rightarrow L$. A periodic driving process is essential to sustain directional motion in space, perform work repetitively, and drive systems further away from equilibrium upon alternating conditions multiple times. To achieve such directional pumping, both kinetic barriers and state's stability must be affected by the alternating condition, i.e., the driving process. This double requirement is known in physics literature as the "No pumping theorem".^[26]

In principle, alternation of any condition can afford a non-autonomous energy ratchet mechanism, provided that the thermodynamic and kinetic conditions outlined above are respected. For example, not only alternating redox^[16,17] or acid/base conditions,^[27,28] but also temperature, humidity, magnetic field, or other parameters could result in conceptually analogous effects. In fact, some of the first purposely-designed energy ratchets featured a combination of orthogonal stimuli.^[29,30] A particularly important kind of driving process is provided by light irradiation, as we now discuss.

2.3. Light-Driven Energy Ratchets

Light can be used as an energy input, and the most common scenario is the use of photoswitches. We will confine our discussion to them, while noting that other approaches have also been explored.^[31,32] In photoswitches, a photon absorption can induce an isomerization, bringing the system away from equilibrium. This is evident when using T-type photoswitches, where light irradiation promotes the formation of a thermodynamically less stable isomer that reverts thermally to the thermodynamic stable one, an important phenomenon for energy storage purposes.^[33,34] Ratchet mechanisms offer the opportunity to transfer part of the energy involved in the photoswitching process, coupling it to other reactions of the networks.

An example of light-driven system leveraging an energy ratchet has been recently reported by the Feringa group, who used light to promote a thermodynamically unfavorable imine exchange reaction.^[35] The authors studied a dynamic covalent cage formed by three aldehyde-terminating azobenzene units, which formed imine bonds with two triamines (Figure 4a). The cage can be isomerized by light of 340 nm, interconverting between (mostly) *EEE-5* and (mostly) *ZZZ-5*. The latter is thermodynamically prone to imine exchange; therefore, addition of 2-methoxybenzylamine **6** affords the open form of *ZZZ-5-6*. Irradiation with a different wavelength (420 nm) or heating

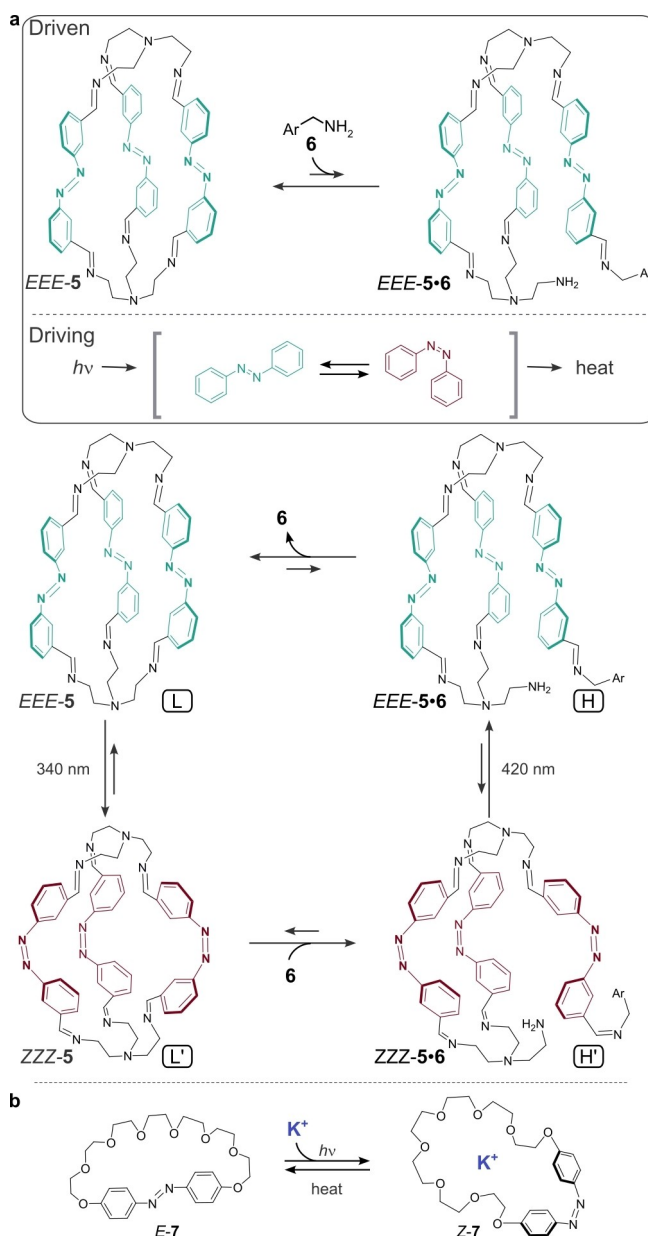


Figure 4. a) Reaction network for a non-autonomous light-driven energy ratchet coupling azobenzene isomerization to the formation of an imine bond. b) Photoreaction having features suitable for an autonomous light-driven energy ratchet mechanism involving metal ion coordination.

reverts the azobenzene units to their *E* isomer, affording *EEE-5·6*. Since in the *EEE* form imine exchange is less thermodynamically favored than in the *ZZZ* form, the system resides in a high energy state, which relaxes to equilibrium over time.

When both isomers of a photochromic compound absorb light of a given wavelength, photoisomerization can be promoted in both directions. For example, both *E*- and *Z*-azobenzene absorb at ca. 400 nm, and therefore light of that wavelength promotes both *E*→*Z* and *Z*→*E* photo-reactions. This effect can be exploited to drive systems away from equilibrium using continuous irradiation. Energy ratchet mechanisms that can operate in this way have photostationary states (PSSs) that are independent of the occurrence of the chemical reaction, while the chemical reaction itself is affected by the photoswitching process. Photoresponsive crown ether **7** (Figure 4b) belongs to this class of molecules.^[36] The observed PSS is independent from the presence of alkali metal cations, and the binding affinity is strongly dependent on the isomerization: in the *E*-isomer the binding constant is negligible, while the *Z*-isomer binds metals with affinities up to 1590 M⁻¹ in the case of K⁺. The effect of continuous irradiation on metal complexation has not been investigated. The features required for autonomous light-driven energy ratchets are somehow uncommon (little influence of chemical reaction on photoreactivity), but there are already reports in the literature of systems that appear to have suitable properties.^[37–39]

2.4. Principles of Light-Driven Energy Ratchets

The fundamental principles at the basis of light-driven systems are different from chemically-driven ones, and we refer readers to detailed articles that clarify their peculiarities.^[40,41] Nonetheless, when considering photoswitches exposed to intermittent light irradiation, it becomes possible to make significant parallels between light- and chemically-driven systems, pointing at common design principles. The simplest case in which a photoswitch can be included in a ratchet mechanism is when photoisomerization changes the equilibrium constant of an associated equilibrium. In such a case, the operating principles of light-driven energy ratchet resemble those discussed in section 2.2. Indeed, it is possible to consider the alternation between two states of a photoswitch in the same way as it was done with different redox states. As a result, one could alternate irradiation with light of two different wavelengths, favoring each of the two isomers alternatively (Figure 5a). The same result can be achieved by alternating irradiation with dark if the employed photoswitch reverts thermally to the ground state (Figure 5b). Light irradiation might also be continuous, affording autonomous ratchet mechanisms (Figure 5c). Leveraging continuous irradiation implies also a different design of the investigated systems, because while in previous cases an ideal photoswitch is one that can be accumulated almost exclusively in one isomer or the other, here PSSs featuring

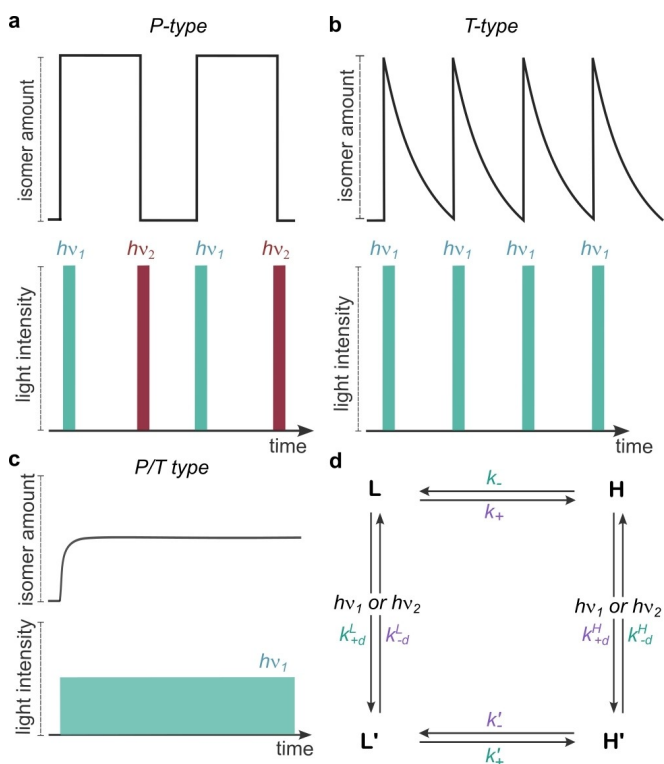


Figure 5. Irradiation conditions that might enable light-driven energy ratchets. In each panel, the top trace indicates the amount of a given photoisomer present in solution, while the bottom trace reports on irradiation conditions. In particular: a) a thermally stable photoswitch (P-type) is converted using light of two different wavelength, alternated with dark intervals; b) a thermally unstable photoswitch (T-type) alternating irradiation with darkness; c) a generic photoswitch is irradiated with a wavelength that can promote both photoreactions. d) Square reaction network featuring two photoreactions and two thermal reactions.

concentrations of the two isomers close to 50:50 seem desirable, because the simultaneous presence of all states facilitates having high speeds at every step of the reaction network. Autonomous energy ratchet mechanisms driven by light have not received much attention from the experimental community, but are very useful to illustrate the principles of autonomous systems. To discuss this mechanism, in the following we consider that the photoreactivity is not affected by the occurrence of coupled chemical reaction, i.e., the PSSs associated with the two photoreactions are identical.

When molecules are continuously exposed to light, absorption and isomerization happen stochastically at the level of single molecules. In other words, the isomerization of an individual molecule^[42] is a random event, which we can estimate the probability of, but we do not control the time at which it happens (contrary to non-autonomous energy ratchet mechanisms described in sections 2.1 and 2.2). At the ensemble level, these stochastic processes can be mathematically treated like chemical reactions, with rate constants defined in terms of tunable external parameters. For instance, in samples having low absorbance, photochemical reactions can be modeled as first-order

reactions depending on parameters such as sample volume, light intensity, absorption coefficient (ϵ) and isomerization quantum yield (QY).^[43,44]

To model a generic light-driven autonomous energy ratchet, we consider the Scheme in Figure 5d and associate a rate constant k_{+d} to processes driving transitions $L \rightarrow L'$ and $H \rightarrow H'$ and a rate constant k_{-d} to driving transitions $L' \rightarrow L$ and $H' \rightarrow H$. Crucially, the ratio $k_{+d}/k_{-d} = K_{PSS(\lambda)}$ reflects the PSS ratio that would be generated by light irradiation in the absence of the horizontal processes for both $[L']/[L]$ and $[H']/[H]$, since their PSSs are identical. This ratio does not depend on the standard chemical potential difference between the species. Continuous light irradiation allows an autonomous driving process to keep the system out of equilibrium, inducing a net chemical current across the network, which will reach a steady state. At steady state, we can quantify the directionality as the ratio between the average frequency at which the network is travelled clockwise over counterclockwise. This quantity is typically referred to as the ratcheting constant K_r ^[45] (also called r or r_0)^[46–48] and can be computed by dividing the product of the rate constants associated with counterclockwise processes (green) by the product of the rate constants associated clockwise processes (purple):

$$K_r = \frac{k_{+d}^L \times k_{+d}^H \times k_{-d}^L \times k_{-d}^H}{k_{-d}^L \times k_{-d}^H \times k_{+d}^L \times k_{+d}^H} \quad (1)$$

This expression of K_r is general for all autonomous systems described by cyclic reaction networks: light-, chemically- and redox-driven ones. What changes case-by-case is the expression of k_d values, the rate constants associated with the driving reaction. In fact, the following sections on physical principles present specific implementations of equation 1. Another general property of autonomous systems is that all the reactions in the cycle are simultaneously away from equilibrium. For example, here both $L \rightleftharpoons H$ and $L' \rightleftharpoons H'$ reactions are kept away from equilibrium in the steady-state, besides the driving reactions. As a rule of thumb, the faster reaction will be closer to equilibrium, while the slower reaction will be further from equilibrium. In the autonomous systems that we will discuss next, we will focus only on the driven reaction that is experimentally determined as far from equilibrium.

Returning to considering the specific case of light-driven systems, when the photoreaction is not affected by the coupled reactions (e.g., $k_{+d}^L = k_{+d}^H$) the k 's associated with driving processes can be simplified to give $K_r = K'/K$. Consequently, directionality is fully controlled by the equilibrium constants K' ($= k_{+}'/k_{-}'$) and K ($= k_{+}/k_{-}$), similarly to the non-autonomous energy ratchet mechanism. When $K' > K$, the ratchet mechanism favors a counterclockwise current; when $K' < K$, the ratchet mechanism favors a clockwise current. When $K' = K$, the system can be described as kinetically symmetric, and its steady state is characterized by the absence of a net cycling current, implying that the horizontal transitions are at thermodynamic equilibrium. When the system is kinetically symmetric, an external driving process may still keep the

vertical transitions out of equilibrium (e.g., at PSS). However, this is not enough to affect the horizontal reactions.

2.5. Spatial Phenomena in Energy Ratchets

Additional opportunities emerge from compartmentalization, and more broadly by introducing some sort of spatial asymmetry. One of the simplest ways of introducing a differentiation in space is to use an electrochemical reaction as the driving one, and two different electrodes to promote it. Experimentally this setup is accessible by using a bipotentiostat. Under such a setup, oxidation and reduction are not alternated anymore in time; instead, it is the diffusion of species between the anode and cathode that provides the necessary delay between oxidation and reduction. Recently, we demonstrated the viability of this experimental setup using a redox-active pseudorotaxane composed of calix[6]arene **8** and alkyl viologen dumbbell **9**²⁺ (Figure 6a).^[49] In literature, also other systems leverage a conceptually similar strategy, to transport ions across membranes or control self-assembly and fiber formation, albeit further studies would be needed to unravel the kinetic details.^[50–52]

In our case, the complex **[9**²⁺**⊂8]** is reduced at the cathode and then disassembles while diffusing to the anode. Oxidation of **9**²⁺ at the anode, self-assembly, and diffusion to the cathode close the cycle. For the self-assembly reactions to be driven away from equilibrium, they must participate in the sequence of reactions involved in electrons moving from the cathode to the anode, e.g., as occurring in the reaction cycle highlighted in green in Figure 6b. Therefore, a key requirement is that the equilibration of the self-assembly reactions should occur before reaching the opposite electrode by diffusion. While this may seem a constraining requirement, taking advantage of mass transport phenomena other than diffusion and modulating the interelectrode distance offer significant flexibility.

When the potentials of the two electrodes are kept constant, the system reaches a steady-state, characterized by a directional chemical current in the reaction network, with both self-assembly reactions being kept away from equilibrium: **[7**²⁺**⊂6]** keeps disassembling close to the cathode, while **7**²⁺ and **6** keep assembling in proximity to the cathode. A peculiarity of this setup is that it offers an alternative to light for realizing energy ratchet mechanisms operating autonomously, i.e., without alternating conditions in time.

The theoretical treatment of spatially-resolved systems brings an increased complexity, due to the interplay between chemical reactions and diffusion. There are two main approaches in the literature to deal with space in chemical systems. The first one treats space continuously by combining mass-action kinetics and Fick's laws of diffusion, resulting in the so-called reaction-diffusion equations. This is the typical treatment used to model pattern formation and waves. The second approach is to introduce

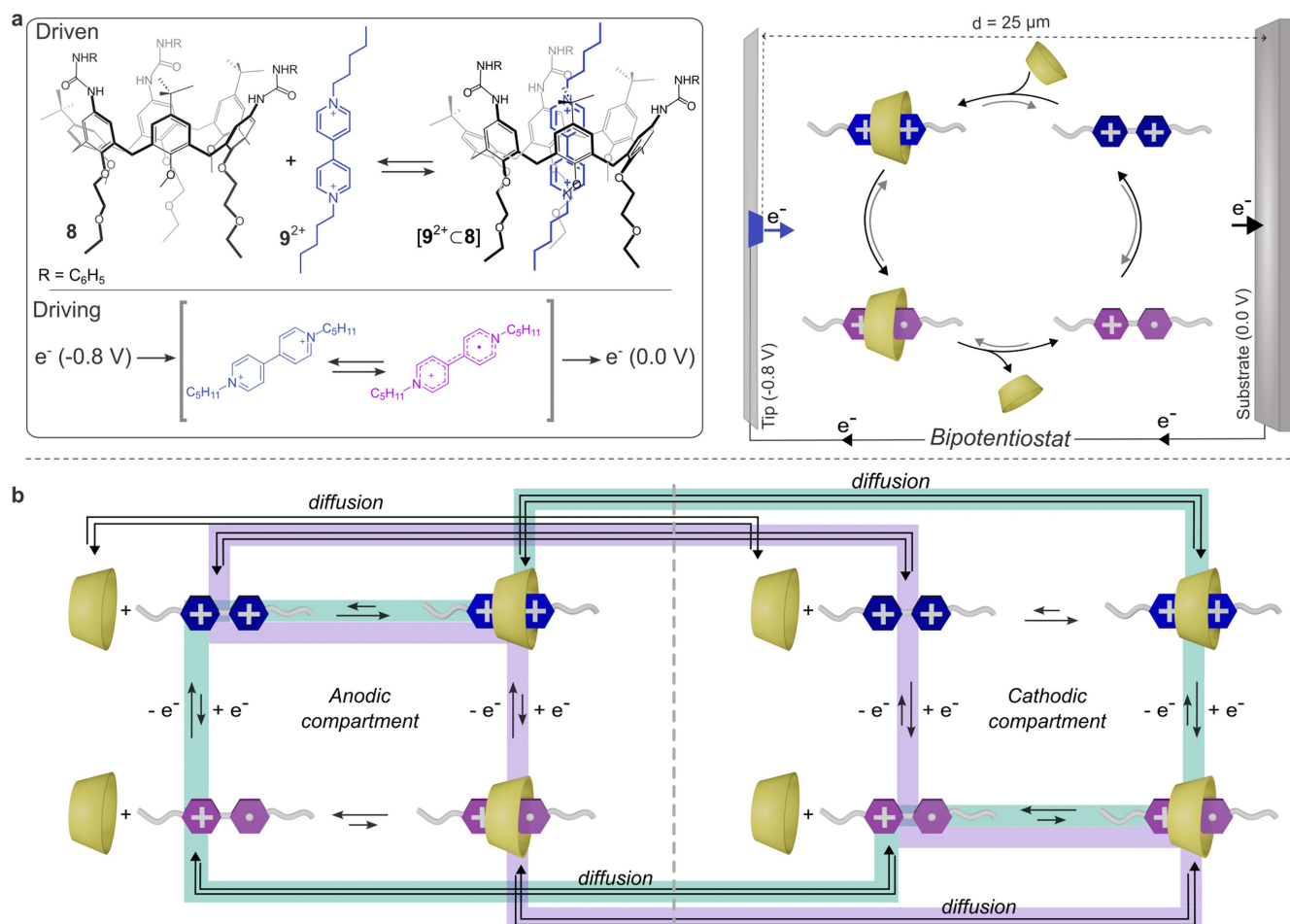


Figure 6. a) Components, experimental setup, and key reactions of an energy ratchet enabled by the simultaneous control of two electrodes separated in space; b) Reaction network that describes chemical reactions and diffusion processes.

compartments. Within this framework, each compartment is treated as a sub-system where concentrations are homogeneous and diffusion is introduced as a set of additional reactions that model how species move from one compartment to the other. Consequently, the size of chemical reaction networks grows as new compartments are introduced.

For example, the redox-active pseudorotaxane just discussed can be described by the network in Figure 6b, which has eight states and thirteen reactions. This often leads to the emergence of multiple cyclic pathways realizing the ratchet mechanism, for example the purple and green ones in Figure 6b. To treat mathematically the interplay between competing cycles, one needs to use graph-theoretical techniques,^[53] the description of which is beyond the scope of this review. However, the general idea is that a given cycle is more relevant the more it is populated, therefore chemical intuition can come to rescue. For example, here the green cyclic sequence of reactions is the one exploited, while the purple one is practically irrelevant, as it involves the oxidation of the complex $[9^+ \cdot 8]$ in proximity of the anode, which is highly unlikely.

The presence of multiple cyclic pathways might also enable emergent phenomena, yet to be explored.

Another general aspect illustrated by this example is that when bimolecular processes such as self-assembly steps are involved in a ratchet mechanism, directionality will in general depend on the concentration at which the system is operated. Therefore, K_r can change and one may need to determine the steady-state concentrations of some of the species before computing it.

3. Information Ratchets

3.1. Chemically-Driven Information Ratchets

Information ratchets operate on principles different from energy ratchets. In an idealized case, they operate under steady-state conditions, thus not relying on any alternation of stimuli, but on harvesting a constant energy supply. For example, a frequent energy source in biological settings is the ΔG associated with the hydrolysis of ATP to ADP. Importantly, this energy is associated with the concentrations of ATP and ADP in the relevant location, and not

with the intrinsic energy of the bond that is broken in the hydrolysis reaction. In other words, energy is available because the concentration of ATP is higher than its equilibrium value. Information ratchets appear widespread in biology, while remaining rare in artificial systems.

To create a parallel with energy ratchets, we start also this section by discussing a case of (pseudo)rotaxane assembly. Here, the assembly is the result of operating an information ratchet mechanism (Figure 7).^[54] Macrocycle **10** can establish only weak interactions with dumbbell **11**, and the equilibrium of the driven reaction is shifted towards the separated components under the typical experimental conditions (high millimolar concentration in organic solvent). The energy-providing reaction is the conversion of Fmoc derivative **12** (Fmoc = 9-fluorenylmethyloxycarbonyl) into 4-nitrophenol (**13**), dibenzofulvene (**14**), and CO₂. This reaction can be promoted by amines in two steps: in the first step, the amine attacks **12** to form a Fmoc-carbamate group and release **13**; in the second step, the intermediate carbamate is deprotonated, releasing **14** and CO₂, as it occurs in classic peptide deprotection. These two steps can be considered analogous to substrate binding and product release in enzymatic catalysis.

Since dumbbell **11** terminates with a Fmoc-protected amino group, the corresponding deprotected precursor can act as a catalyst. The peculiarity of this system is that the first step of the catalyzed driving reaction, i.e., carbamate formation, is faster when the macrocycle surrounds the primary amine (state H') with respect to the macrocycle being free in solution or onto the collecting chain. The observed preferences originate from the stabilization of

transition states, as confirmed in related studies.^[55,56] On the contrary, the second step is faster when the macrocycle is not surrounding the carbamate, being either in solution (state L) or onto a collecting chain. Ideally, in the absence of side reactions and complete selectivity (referred to as a perfect doubly kinetically gated system),^[57] the only catalytic reaction sequence that is available for the conversion of **12** into products is H'→H→L→L'. In such a sequence, macrocycle dethreading (or relocation onto the collecting chain) is coupled to substrate-to-product conversion, as the two reactions happen together—here sequentially from the mechanistic point of view. Therefore, under continuous substrate turnover, the population of species does not reflect the thermal equilibrium of self-assembly reactions. In this particular case, the slowest step of the chemical reaction cycle is the dethreading from state H, to the point that it is completely prevented by the bulky Fmoc terminal under the operating condition: relocation onto the collecting chain is favored and results in the accumulation of target high-energy rotaxanes.

In analogy with the energy ratchet-based molecular pump described in the previous section, suitable engineering of an intermediate-size speed bump—here the -CF₃ group—is key in enabling directional motion and progressive driving of the system away from equilibrium. After carbamate formation (the first step of the catalyzed reaction), relocation of the macrocycle onto the collecting chain becomes favored because the carbamate is a poor station compared to triazoles. The co-conformational^[58] rearrangement is associated with a more efficient Fmoc removal, preparing the dumbbell for a new reaction cycle.

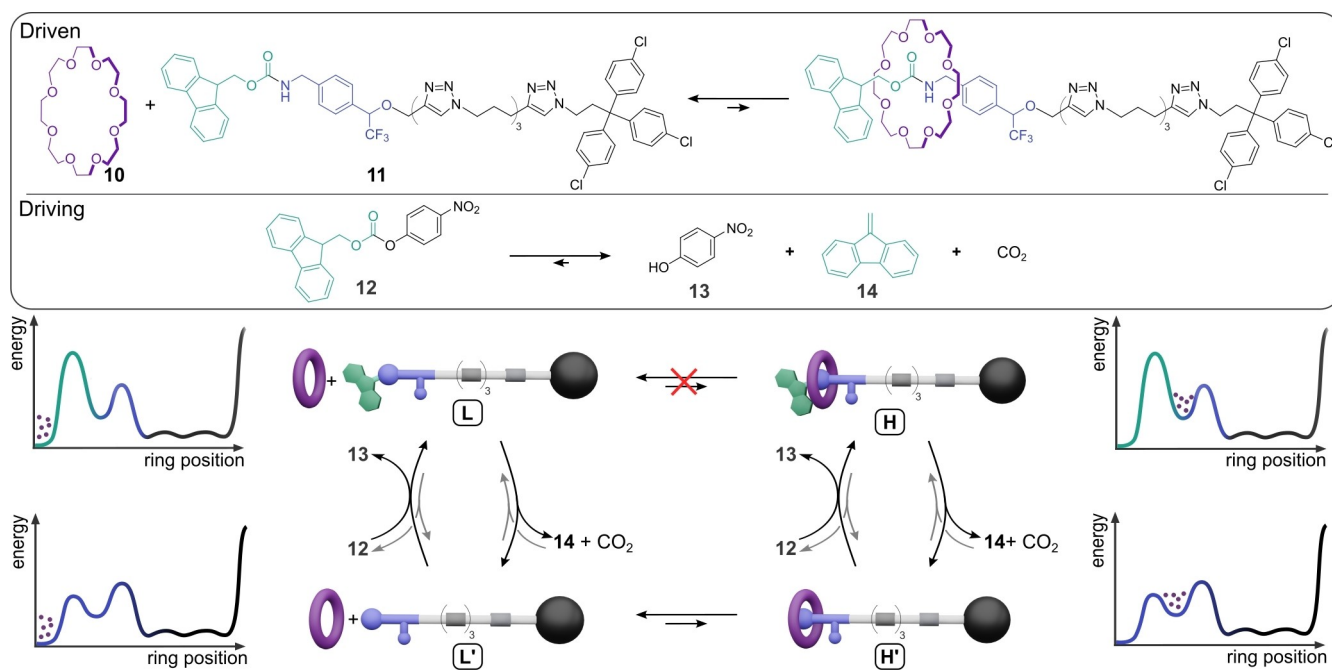


Figure 7. Chemical reaction network and potential energy surfaces associated with the formation of a high-energy pseudorotaxane, enabled by a chemically-driven information ratchet. The scheme focuses on Fmoc-protected species because these are the species detected by mass spectrometry in the experimental conditions employed for autonomous operation. The red cross indicates that the reaction is exceedingly slow under the employed experimental conditions.

The $-\text{CF}_3$ barrier is sufficiently high that loading another macrocycle is kinetically favored over dethreading from the collecting chain. Under continuous consumption of **12** the cyclic reaction sequence could be repeated multiple times, allowing the autonomous formation of a [4]rotaxane.

An important class of information ratchet mechanisms is constituted by reactions involving coupling agents, such as carbodiimides. A remarkable example is the conversion of carboxylic acids to carbonyl compounds typically not stable in water, such as anhydrides and esters. In an epitomic case developed by Boekhoven and Hartley, the reaction to be shifted is the coupling of diacids such as aspartic acid derivatives **15** to form the corresponding anhydrides **16** (Figure 8a).^[59,60] The reaction providing energy for this transformation is the hydration of carbodiimide **17** to give urea **18**, which is catalyzed by acids. When acid **15** promotes the reaction, the catalytic cycle looks like the one in Figure 8a. When this reaction occurs in water, the equilibrium of the driven reaction is shifted towards the diacid: carbodiimide hydration reaction transfers part of its energy to enable the formation of a high-energy anhydride

that decays over time, implying the presence of a ratchet mechanism. The reason why it is less immediate to associate this reactivity to ratchet mechanisms is that—unlike most cases of molecular ratchets—the products of the driven reaction (anhydride **16** and H_2O) cannot promote the opposite coupled reaction, which would be carbodiimide hydration coupled to anhydride hydrolysis. Essentially, the carbodiimide can only bind to the reagent of the driven reaction, i.e., diacid **15**. In more general terms, when a catalytic process occurs conditionally to a modification of the catalyst, such as a conformational change, it implies the presence of an information ratchet mechanism driven by chemical energy.

Carbodiimide-driven systems are of high current interest, being widely employed to form transient systems, from small molecules to materials.^[59–64] An elegant example that took advantage of the carbodiimide chemistry has been reported by the Leigh group, which used this type of chemistry to obtain a unidirectional rotary motor.^[65] The machine can be described by the square reaction network depicted in Figure 8b. Diacid **19** is axially chiral and it thermally enantiomerizes. As an acid, it can also catalyze carbodiimide hydration, affording anhydride **19'**, which can also enantiomerize. The first peculiarity is that racemization occurs via two different barriers (COOH over H in the acid state vs. anhydride flipping in the other case). The second peculiarity is that when a chiral carbodiimide is used, anhydride formation is faster in the $(-)$ -**19** state with respect to $(+)$ -**19** state. Moreover, when the chiral catalyst (*R*)-cat is used for anhydride hydrolysis, the hydrolysis is faster in the $(+)$ -**19'** state with respect to $(-)$ -**19'**. As a result, the cyclic sequence $(-)$ -**19** \rightarrow $(-)$ -**19'** \rightarrow $(+)$ -**19'** \rightarrow $(+)$ -**19** occurs preferentially over the reverse cyclic sequence, and is associated with the unidirectional rotation of the phenyl ring.

This rotor contains two ratchet mechanisms. The first involves anhydride formation and hydrolyses in states having the same chirality, according to a cyclic reaction network analogous to the one presented in Figure 8a. The second one also involves anhydride formation and hydrolysis, but in this case the two steps occur from states having opposite chirality, ultimately affording the unidirectional exploration of the square reaction network depicted in Figure 8b, due to their different kinetic selectivity in the enantiomeric states.

Using carbodiimides to promote anhydride (or ester) formation followed by hydrolysis is an effective approach to obtain the simultaneous formation and destruction of chemical bonds, which was recognized as an essential feature in the design of non-equilibrium systems.^[66–68]

Another element highlighted by this rotor is the source of asymmetry. In this case, the rotor itself has two enantiomeric forms, and it is the carbodiimide energy source that—being chiral—results in diastereomeric transition states, thus different reactivities of the enantiomers. Similarly, a chiral anhydride catalyst affords another diastereomeric pair associated with the hydrolysis step. In (pseudo)rotaxanes the source of asymmetry often arises from a structural asymmetry of the dumbbell, as in previous

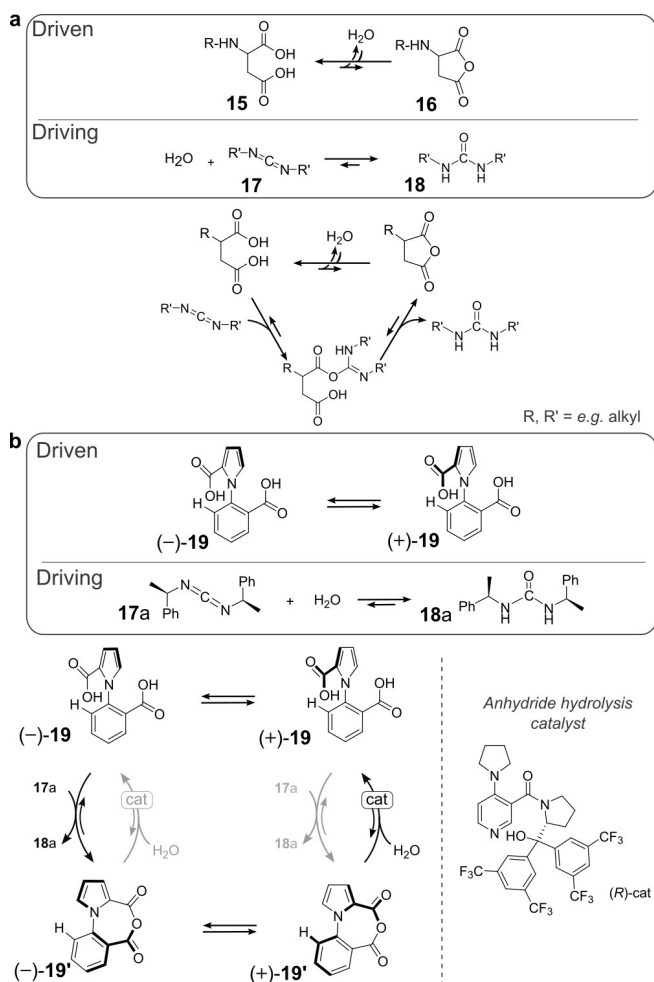


Figure 8. a) Reaction network that can be used to rationalize anhydride formation as an endergonic process powered by carbodiimide hydration; b) reaction network in which carbodiimide hydration is employed to power a unidirectional rotation process.

and other examples.^[69] The macrocycle itself can act as source of asymmetry, as nicely demonstrated by Vives, Sollogoub, and co-workers.^[70]

3.2. Principles of Chemically-Driven Information Ratchets

In a minimalist chemically driven information ratchet, the vertical transitions in Figure 9a are associated with an exergonic reaction converting a substrate S into a product P, that can be catalyzed by either L ($S+L\rightleftharpoons L'+P$) or H ($S+H\rightleftharpoons H'+P$). Consistently with the whole manuscript, all reactions are considered reversible, implying that e.g., also the binding of P to H to afford H' might take place. Reconsidering equation 1 in this context, the rate constants associated with each vertical transition are then given by the sum of the rate constants of two different chemical reactions: $k_{+d}^L = k_{+S}^L[S] + k_{+P}^L[P]$ for the transition $L\rightarrow L'$, $k_{-d}^L = k_{-S}^L + k_{-P}^L$ for the transition $L'\rightarrow L$, $k_{+d}^H = k_{+S}^H[S] + k_{+P}^H[P]$ for the transition $H\rightarrow H'$, and $k_{-d}^H = k_{-S}^H + k_{-P}^H$ for the transition $H'\rightarrow H$.

The rate constants of the chemical reactions cannot have any arbitrary value, because there are some constraints to be respected, imposed by microscopic reversibility. One constraint is that any reaction cycle (not associated with energy consumption) must be equally likely to be travelled clockwise or counterclockwise. Mathematically, the ratio of clockwise (purple) and counterclockwise (green) rate con-

stants should be equal to one. For example, for the cycle associated with binding of S, switching, and release of S we have:

$$\frac{k_{+S}^L \times k_{+}^L \times k_{-P}^H \times k_{-}^H}{k_{-S}^L \times k_{-}^L \times k_{+P}^H \times k_{+}^H} = 1 \quad (2)$$

At the same time, the cycle associated with binding of P, switching, and release of P has its own microscopic reversibility constraint, expressed with:

$$\frac{k_{+P}^L \times k_{+}^L \times k_{-S}^H \times k_{-}^H}{k_{-P}^L \times k_{-}^L \times k_{+S}^H \times k_{+}^H} = 1 \quad (3)$$

The last microscopic reversibility constraint associated with the network of Figure 9a is that the equilibrium constant of the $S\rightleftharpoons P$ reaction must be the same if we calculate it using the catalytic cycle associated with L or H, which is mathematically expressed by:

$$\frac{k_{+S}^L}{k_{-S}^L} \times \frac{k_{-P}^L}{k_{+P}^L} = \frac{k_{+S}^H}{k_{-S}^H} \times \frac{k_{-P}^H}{k_{+P}^H} \quad (4)$$

It is important to consider such constraints when performing kinetic modeling of nonequilibrium systems, because overlooking them may lead to incorrect conclusions.^[71]

Microscopic reversibility constraints can be used to simplify the expression of the ratcheting constant computed with equation (1). A popular choice among theoreticians is to obtain, after some algebraic passages:^[48]

$$K_r = \frac{\frac{k_{+S}^L e^{-\Delta G/RT+1}}{k_{-P}^L} \times \frac{k_{-S}^H+1}{k_{-P}^H}}{\frac{k_{-S}^L+1}{k_{+P}^L} \times \frac{k_{+S}^H e^{-\Delta G/RT+1}}{k_{-P}^H}} \quad (5)$$

The reason why this formulation is popular is that it illustrates better than other mathematical expressions two general features of catalysis-driven ratcheting.

First, any ratchet mechanism requires an energy source to operate. The energy is provided by $\Delta G \neq 0$ for the conversion of S to P. When $\Delta G = 0$ ($e^{-\Delta G/RT} = 1$), numerator and denominator of each of the main fractions become equal, and thus $K_r = 1$ for any value of the rate constants—directionality cannot emerge. For instance, in Figure 7, the thermodynamically unfavored assembly of a high-energy rotaxane is enabled by the coupled catalytic conversion of **12** into lower-energy products, providing the necessary free-energy source.

The second general feature is that the stability of states, i.e., the equilibrium constants of threading reactions (K and K'), have no role in determining the directionality of the system, indeed they do not appear in equation (5). When $\Delta G \neq 0$, the directionality is controlled by the rate constants of the catalyzed reaction, which instead appear in equation (5). In particular, it can be demonstrated that directionality only depends on the difference between transition states' free energies, a purely kinetic phenomenon.

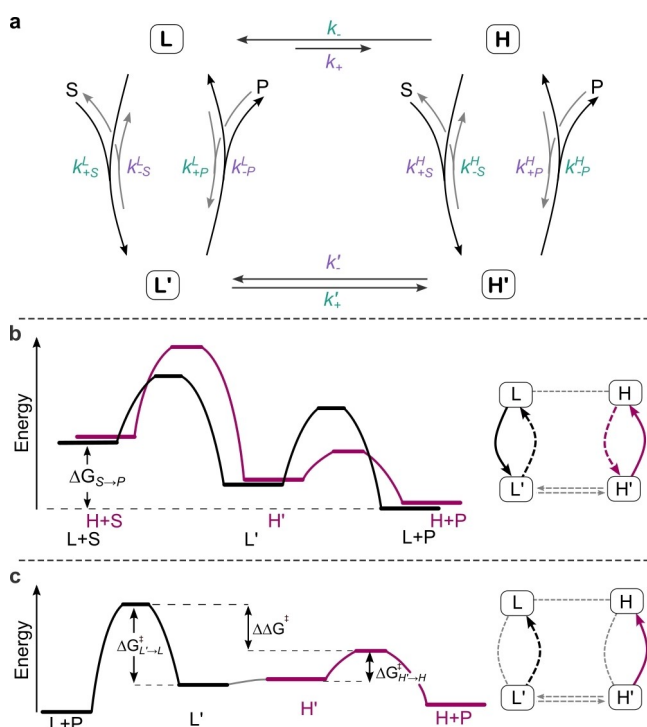


Figure 9. a) Reaction network underlying a chemically-driven information ratchet. b) Energy profiles associated with the catalytic conversion of S into P by catalysts L or H; c) energy profiles associated with L' and H' kinetic resolution to give P. A similar profile can be drawn for the kinetic resolution to give S (not represented).

To rationalize this finding in terms possibly more familiar to experimentalists, we find two strategies particularly useful. One strategy is to consider the properties of L and H as catalysts. For example, we focus on L and consider the propensity to populate L over the enzyme-substrate complex L', which is controlled by rate constants k_{-S}^L, k_{-P}^L vs k_{+S}^L, k_{+P}^L . If product formation is practically irreversible, as in most experimental cases, we can neglect k_{+P}^L . By making this simplification one recovers the Michaelis–Menten parameter of enzyme L: $K_{MM}^L = (k_{-S}^L + k_{-P}^L)/k_{+S}^L$. When $k_{-S}^L \gg k_{-P}^L$ (slow product formation), one can think at the Michaelis–Menten parameter in terms of a thermodynamic quantity. Besides this limiting case, the parameter has a kinetic interpretation, as it reflects the propensity of an enzyme to be bound to a substrate at the steady-state: the lower K_{MM}^L the more associated the enzyme is. In the simplest scenario, one can imagine a similar stability for $L \rightleftharpoons H$ and $L' \rightleftharpoons H'$, but the Michaelis–Menten parameter being lower for L than for H. This situation implies that there is a higher propensity to populate L' at the steady-state with respect to H'. Therefore, catalysis will continuously overpopulate L' with respect to H', preventing the equilibration of L' and H' and simultaneously leading to the emergence of a directional current. The energy diagrams in Figure 9b exemplify this scenario, highlighting that substrate binding is favored for L, while product release is favored in H'. Therefore, in efficient molecular information ratchets, the components operate as a bistable catalyst that switches during the catalytic cycle. Importantly, such catalytic cycle results in a chemical current from L to H through the path $L \rightarrow L' \rightarrow H' \rightarrow H$. As occurring for energy ratchets, the overall reaction associated with this sequence of steps corresponds to the sum of the driving and driven reaction.

An alternative rationalization strategy is recognizing that the role of transition states is analogous to the Curtin–Hammett principle in physical organic chemistry, where the difference of free energy between transition states dominates the outcome of kinetic resolutions, rather than the difference of stability between the reactants.^[72] For example, once the substrate has bound the catalyst, L' and H' interconvert, and releasing the product by reverting to H is faster than releasing it by reverting to L, because the associated transition state is lower. One can consider this process as a dynamic kinetic resolution of L' and H', affording H (Figure 9c). This effect was engineered in pioneering works where the co-conformational equilibrium of a rotaxane was biased: a non-equilibrium distribution was obtained by installing a stopper along the dumbbell, blocking shuttling via a dynamic kinetic resolution process.^[73] To obtain a full ratchet, one should engineer such a resolution effect for both reactions. This is indeed the case for the system in Figure 7, where binding of the substrate occurs preferentially (lower transition state) in the disassembled state, while the product release occurs preferentially in the assembled state. The overall directionality is solely dictated by energy differences in transition states.

At the same time, the state's stability can influence the efficiency of information ratchet operation. Indeed, if a

given state is thermodynamically very stable, it will act as a sink, slowing down other reactions. This concept was nicely illustrated in the domain of chemical catalysis by Kozuch and co-workers, who showed that the overall speed of a given catalytic process is governed by the difference in energy between the most stable intermediate and the least stable transition state of the catalytic cycle.^[74,75] Analogous principles apply to autonomous non-equilibrium systems.^[76]

The role of state stability becomes even more significant when considering experimental practice. Indeed, it is well established that for many organic reactions the transition state shares some features of the species (reactant or product) that is closer in energy. This relation is known as Hammond's postulate. As a result, in the experimental practice a chemical modification that is supposed to affect the thermodynamic stability of a given state may well be influencing a transition state. These considerations suggest carefully evaluating case-by-case how changes in the molecular design affect the operation of a ratchet mechanism, being guided by theory while not overlooking the complexities presented by real systems.^[57,72,77]

3.3. Light-Driven Information Ratchets

Light can also be used as energy source to drive an information ratchet. Photoactive rotaxane **20** (Figure 10a) is considered the first information ratchet by design.^[78] Under irradiation, it accumulates rings on one of the two stations available, so that the co-conformational distribution is affected. Indeed, rotaxane **20** includes a photoswitchable stilbene unit in the dumbbell. Stilbene isomerization can be promoted by the benzophenone unit present on the macrocycle, but this sensitized isomerization is dependent on the location of the macrocycle. In particular, the photoreaction from *Z*- to *E*-stilbene is more efficient when the macrocycle is close to the stilbene. Since ring shuttling is prevented when stilbene is in the *Z*-configuration, under continuous irradiation, rings accumulate on the station far from the stilbene unit. In this particular scenario, one can think of this effect as a Le-Chatelier-like shift in the equilibrium populations, in which the relative population of *Z*- and *E*-isomers in the two co-conformations is dictated by the PSSs rather than thermodynamic properties.

The chemical reaction network associated with photoactive rotaxane **20** can also be found in other molecular systems, for example, it underlies molecular switch **21**.^[79] This photoactive system features a bicyclic structure and incorporates two photoswitches. The structure itself is chiral, and it was shown that enantiomerization can occur when the two azobenzenes adopt a *Z*- configuration, while it is too slow in the *E*- configuration. Essentially, this affords the chemical reaction network shown in Figure 10b, which maps closely the one of rotaxane **20**. In this case, the photo-reactivity can become different for the *R* or *S* enantiomers by using circularly polarized light (CPL). For example, when using *r*-CPL the formation of *S*-*EE*-**21** is favored. Here, accumulating a given enantiomer implies the occurrence of a photoresolution, which is the context in which the work was

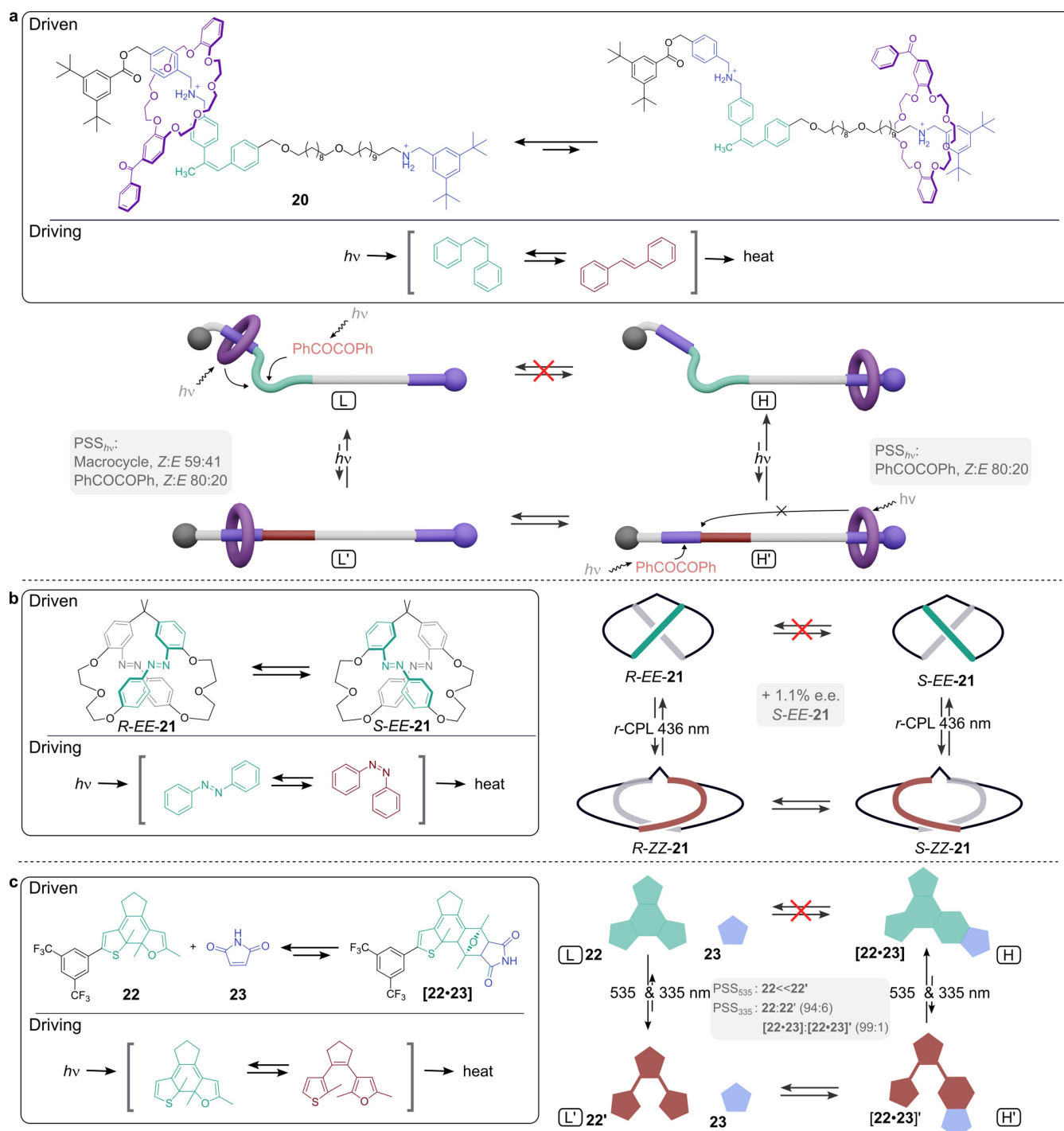


Figure 10. Examples of light-driven systems that operate according to an information ratchet mechanism. a) A rotaxane in which co-conformations are shifted; b) a chiral macrocycle that can de-racemize; c) a small molecule that can form a dynamic covalent bond. The red crosses on top of reaction arrows indicate that the reaction is exceedingly slow under the employed experimental conditions.

presented: by using *r*- or *l*-CPL the authors could obtain a photoinduced e.e. of 1.1% of either of the enantiomers, depending on the circular polarization used. The same principle was also used later on in conceptually similar macrocyclic analogs having planar chirality.^[80] Pioneering work in this area employed overcrowded alkenes, in which photoisomerization switches helical chirality simultaneously.

As a result, the reaction network is even simpler with respect to the above examples, having just a photoreaction that interconverts two enantiomers. Using CPL, an e.e. of 0.07% was obtained.^[81]

Hecht and co-workers used the principles of light-driven information ratchets to control a dynamic covalent reaction. The authors used diarylethene **22**, in which one of the two

aryls is a furyl residue (Figure 10c).^[82] This scaffold can undergo Diels–Alder reactions with maleimide (**23**), while remaining photoswitchable. However, since photocyclization removes the diene functionality of the furyl residue, the closed form cannot react with maleimide to form the respective Diels–Alder adduct. The resulting scheme maps closely those previously described, with two photochemical steps connected by a thermal step. Here, the difference in photoreactivity (different PSS) arises because the two partners of the Diels–Alder reaction have different absorption spectra and QYs when bound or not. For example, when the system is irradiated simultaneously with 335 nm and 535 nm light, the PSS of the adduct is more shifted towards ring closure with respect to the separated components, because only **22** absorbs light at 535 nm (and opens), and not [**22**·**23**]. Therefore, the Diels–Alder adduct accumulates with respect to the dark reaction (e.g., +83% when operating at 25°C). On the contrary, irradiating at a different wavelength (375 nm) can promote ring closure of the unreacted diarylethene **22'**, depleting the adduct concentration with respect to the dark reaction (e.g., –40% at 40°C). The same strategy was employed to photorelease maleimide under physiological conditions and expanded to dynamic covalent C=N condensation/hydrolysis.^[83,84]

Ultimately, all these examples share the same type of chemical reaction network, which is associated with a conformational rearrangement, a racemization process, or a chemical reaction. It becomes then natural to extend this rationalization to other reactions. For example, a class of systems that might operate according to similar principles are photoactive supramolecular polymers. However, such systems are not discrete anymore (even in a simple scenario, there will be a distribution of polymer lengths), which complicates a detailed analysis. Still, some photoactive supramolecular polymers displayed features that are not compatible with equilibrium polymerization, such as strain-driven disassembly.^[85] When considering if a system including photoswitches might display behaviors arising from ratchet mechanisms, it can be useful to keep in mind that information ratchet mechanisms operate under constant irradiation, as they require the irradiation time to be at least in the range of the thermal reactions. Therefore, great care should be taken when operating light-switchable systems under continuous light irradiation, as information ratchet mechanisms might become active. In particular, photoswitches having rapid thermal relaxation are often operated under continuous irradiation, to maintain a metastable state: it might be possible that in some experiments ratcheting effects were present even when not designed.

3.4. Principles of Light-Driven Information Ratchets

To discuss the physical principles underlying light-driven information ratchets, we consider again the network in Figure 5d, but rule out any possible energy ratchet effect by considering the specific case in which $K' = K$. In this scenario, the only possibility to generate kinetic asymmetry in the system is to differentiate the vertical transitions in

Figure 5d, such that species L and L' interact with light differently than species H and H'. For instance, the conversion from L to L' should be more effective than from H to H', where “more effective” implies that the PSS is richer in L' than L with respect to H' and H. As we anticipated in section 2.4, the rate constants associated with the photochemical driving process— k_d —are not constrained by microscopic reversibility and reflect the PSS composition. This relation can be expressed mathematically, for example considering L:

$$\frac{[L']_{PSS}}{[L]_{PSS}} = \frac{k_{+d}^L}{k_{-d}^L} = \frac{\epsilon_L \times QY_{L \rightarrow L'}}{\epsilon_{L'} \times QY_{L' \rightarrow L}} = K_{PSS(\lambda)}^L \quad (6)$$

An analogous relation holds for H. In the specific case of $K' = K$, we can use these relations to simplify the expression of K_r , in equation 1, which becomes $K_r = K_{PSS(\lambda)}^L / K_{PSS(\lambda)}^H$. In contrast with the energy ratchet mechanism, here system's directionality is fully controlled by the photoreactions. For example, in all experimental cases presented in Figure 10 $K_{PSS(\lambda)}^L > K_{PSS(\lambda)}^H$ (the PSS of L is richer in L'), and systems reach a steady state characterized by a counterclockwise current. In other words, considering the bulk speed of photoreactions, when the isomerization of species L is faster than species H ($k_{+d}^L > k_{+d}^H$) and/or species H' isomerizes faster than species L' ($k_{-d}^H > k_{-d}^L$), directionality emerges. This situation is reminiscent of the original Maxwell's Demon thought experiment as the system interacts more quickly with the driving energy source if doing so favors counterclockwise progression. In this sense, information is encoded in species' reactivity: the analogy with Maxwell's Demon has indeed been used to describe the operation of rotaxanes such as **20** (Figure 10).

3.5. Spatially Resolved Information Ratchets

Information ratchets and spatially resolved phenomena are somehow tightly related. Even the inspiring thought experiment of Maxwell's Demon stems from a compartmentalized system. The role of information ratchets in regulating macroscopic scale spatial phenomena is starting to emerge, specifically in relation to chemotaxis. Chemotaxis is the directional movement in response to a gradient of chemical species, and several possibilities have been envisioned to explain this phenomenon, including kinetic asymmetry.^[86–88]

Following the work of Astumian and Sen, we consider an enzyme E that can diffuse between two different locations, having different concentrations of S and P (a gradient, Figure 11). The reaction network is again a square, with $K' = K$ since the horizontal reactions are now diffusion processes. Asymmetry in an analogous network was rationalized considering the Michaelis–Menten parameters in section 3.2. Here, the kinetic constants are the same for both locations, but [S] and [P] have different values, which can still lead to directional cycling in the network ($K_r \neq 1$). If the diffusion coefficients of E and E' are different, the preferential diffusion of E' in one direction is not counterbalanced by the diffusion of E in the opposite direction, and chemo-

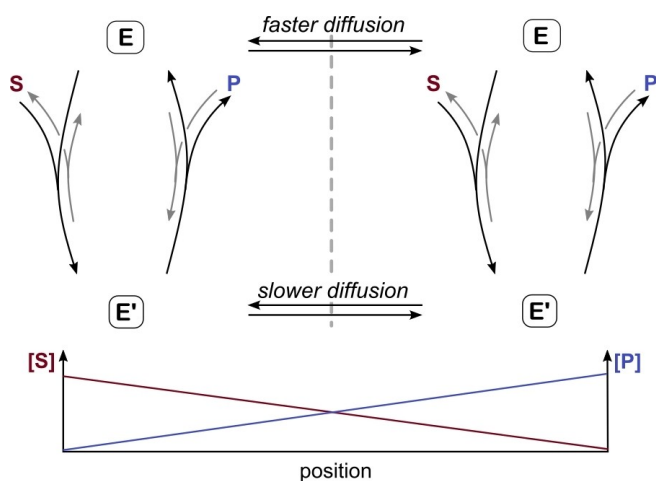


Figure 11. Schematic representation of catalysis-driven chemotaxis of enzyme E enabled by an information ratchet mechanism that exploits a concentration gradient of S and P.

taxis emerges. Thus, a difference in diffusion coefficients and concomitant kinetic asymmetry are both necessary to realize chemotaxis leveraging this mechanism, which can be compatible with some of the experimental evidence associated with enzyme chemotaxis, as the authors have shown using numerical simulations.

This description of chemotaxis gives also a blueprint for the realization of primary active transport and phototaxis. Indeed, if we imagine the dashed line in Figure 11 as a semipermeable membrane, or consider a photoreaction with different PSS as driving process, the same kinetic scheme can be used to envision these phenomena.

4. Generalizations

In previous sections, we discussed clear-cut examples of energy or information ratchets. We also considered steady-states or fully equilibrated systems to describe general physical principles. However, the reality of chemical experiments is usually more complex. In this section we discuss cases of interplays between energy and information ratchet mechanisms.

4.1. Coexisting Energy and Information Ratchets

The simplest cases in which both energy and information ratchet mechanisms coexist are light-driven systems. One of these cases is the light-driven pump formed by macrocycle **24** and dumbbell **25** (Figure 12).^[89] In this system, an azobenzene unit is embedded into the dumbbell. As we have seen occurring in systems driven by pure energy ratchet mechanisms, here isomerization changes the stability of the pseudorotaxane comprised by the axle and a crown-ether. This effect alone would lead to a counterclockwise chemical current in the cycle depicted in Figure 12. At the same time, the PSS is richer in the Z-azobenzene when the ring

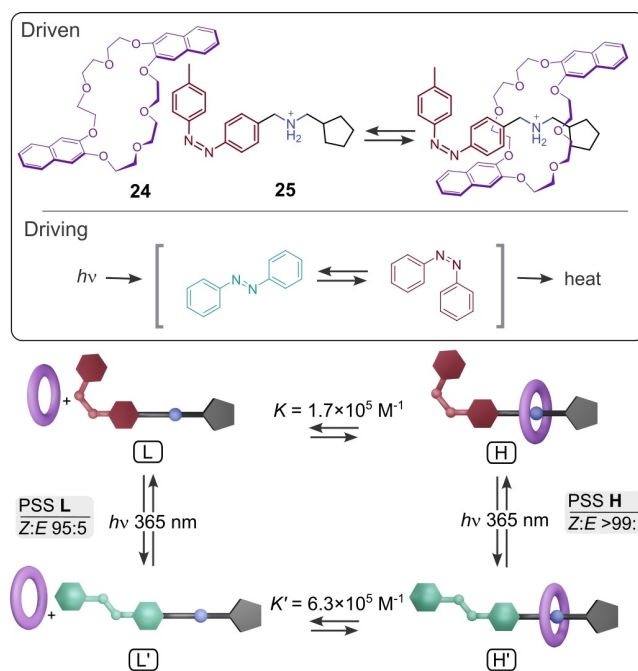


Figure 12. Chemical reaction network associated with the formation of a high-energy pseudorotaxane, enabled by a mixed energy and information ratchet mechanism powered by light.

encircles the dumbbell. Such a difference in PSS composition is characteristic of information ratchet mechanisms, and also promotes a counterclockwise chemical current, being synergic to the energy ratchet component. The information ratchet component depends on the irradiation conditions (as it depends on ϵ and isomerization QY), whereas the energy ratchet component is independent of the irradiation conditions. Having access to all the rate constants characterizing the system, including those of photochemical reactions, allows to quantify the two components. In that particular case the overall ratcheting was composed by 25 % energy ratchet and 75 % information ratchet.^[42] As occurring for the other pseudorotaxanes described, directionality of the network is then coupled with an evident directionality in space.

Significant differences in thermodynamic properties and PSSs have also been observed in phoswitchable supramolecular cages.^[90] For example, cages incorporating or encapsulating azobenzene derivatives could overpopulate less stable structures under irradiation.^[91,92] These effects seem consistent with the operation of mixed energy and information ratchet mechanisms.

A widely employed class of molecules that exploits both an energy and an information ratchet mechanism is the one comprising the rotary motors developed by Feringa, such as the derivative shown in Figure 13.^[93,94] A peculiarity of this system is that photoisomerization inverts the helicity, which governs the thermodynamic stability. Therefore, (*M*)-Z-**26** is more stable than (*P*)-Z-**26**, but upon photoisomerization forms (*P*)-E-**26**, which is less stable than (*M*)-E-**26**, pointing at an energy ratchet component. At the same time, the PSSs associated with the conversion of (*M*)-Z-**26** and (*P*)-Z-**26** to the respective E-isomers are different, favoring (*P*)-E-**21**

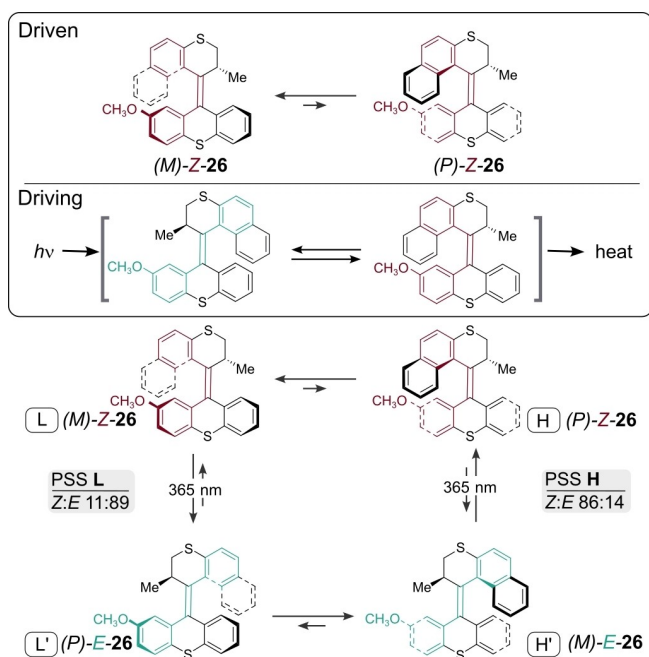


Figure 13. Overcrowded alkene operating as a light-driven rotary motor, featuring both information and energy ratchet effects.

and (*P*)-**Z-26**, respectively. This effect points at an information ratchet component. Some cross-photoreactions have also been observed, indicating an underlying network complexity, but still, it is possible to rationalize the operation of this particular motor and several analogs as a mixed energy and information ratchet. A key structural element for such rotors is the stereogenic carbon atom, which results in different properties for (*P*) and (*M*) isomers by establishing a diastereomeric relation between them. The same group has overcome the necessity for the stereogenic carbon, leveraging supramolecular interactions. In particular, the new rotor is based on an achiral stiff-stilbene photoswitch bearing two urea units.^[95] Isomerization affords two helical isomers that rapidly interconvert at room temperature. Addition of a chiral phosphate derivative forms diastereomeric complexes, upon interaction of the phosphate with urea moieties, thus breaking the chiral symmetry of the system. Indeed, photoreactions were marginally affected by complexation, while circular dichroism and computational data indicated a significant preference for one of the diastereomeric pairs. As a result, a unidirectional chemical current can arise, enabled by an energy ratchet mechanism. The supramolecular control on directionality enabled reversing the direction of rotation just by adding the enantiomeric form of phosphate salt.

Chiral overcrowded alkenes are pioneering examples of artificial molecular ratchets. Remarkably, the rotary motors developed by Feringa and co-workers are among the few molecular ratchets that are capable of transducing the energy harvested, for example by rotating another bond synchronously, contracting gels, and entangling molecules.^[96–102]

For the light-driven mixed ratchets discussed, K_r can be calculated from equation 1. In contrast with pure energy or information ratchet mechanisms, both PSS and equilibrium constants remain important, resulting in:

$$K_r = \frac{K_{PSS(\lambda)}^L \times K'}{K_{PSS(\lambda)}^H \times K} \quad (7)$$

In light-driven systems, when energy and information ratchet mechanisms coexist, it is desirable that both lead to cycling in the same direction, otherwise they might cancel out. Both the pump and rotor described above (Figures 12 and 13) feature energy and information ratchet effects promoting the same directionality.

Spatially-resolved irradiation is also a convenient mean for having coexisting ratchet mechanisms. In principle, to install an information ratchet effect it is sufficient to irradiate only a sector of a given system containing a photoswitch, so that its PSS becomes different in space. Prins and co-workers built on this idea to study anionic azobenzene **27**, which interacts with cationic monolayers of nanoparticles **NP**, with higher affinities when in its *E*-isomer compared with *Z*-isomer (Figure 14).^[103] The difference in affinities of a photoswitch points to an energy ratchet effect. The system was studied in an agarose gel matrix, so that mass transport between different sectors of the gel could be controlled solely by diffusion. Combining isomerization, monolayer binding, and diffusion between an illuminated and a dark sector, affords an eight-state network. The network is similar to the one shown in Figure 6b, but now the driving reactions are photochemical, therefore not subject to microscopic reversibility: energy and information ratchet effects can coexist even at the steady-state. For

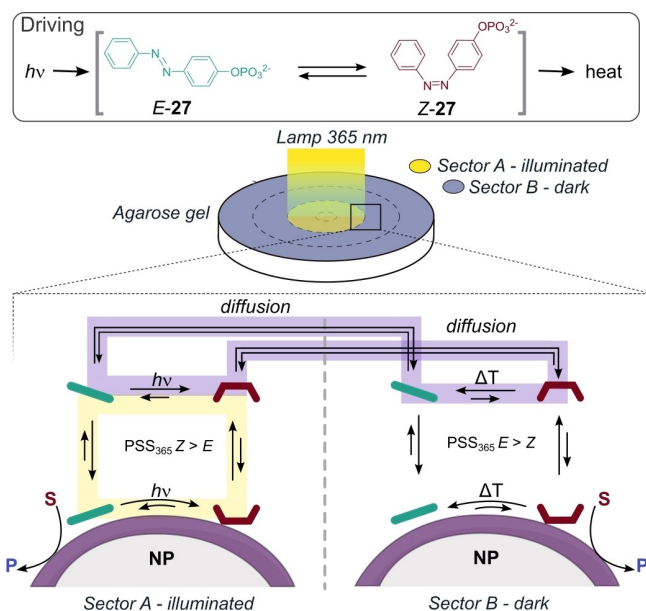


Figure 14. Experimental setup and reaction network that is associated with a spatially-resolved enhancement of catalytic activity promoted by light. The cyclic pathways highlighted in purple and yellow are associated with information and energy ratchet effects, respectively.

example, we can identify an energy ratchet in the sequence of reactions highlighted in yellow, where the PSSs are the same and the equilibrium constants are different. At the same time, we can identify an information ratchet in the purple-highlighted cycle, which includes photoreactions with different PSS, while diffusion constants are the same.

Under continuous irradiation, *Z*-**27** accumulates in sector A, and since it has a low affinity for NP, the monolayer becomes more accessible. The employed nanoparticles can catalyze the hydrolysis of an RNA model substrate, but only when their surface is accessible. Therefore, accumulation of low-affinity *Z*-**27** is accompanied by an enhancement of catalysis. This effect is further increased by the fact that in sector A the substrate is converted to product, and therefore diffusion of more substrate from sector B to sector A is not counterbalanced by the opposite process. Control experiments have shown that continuous irradiation is necessary to observe the nonequilibrium behavior, and the same strategy can be used to induce a local accumulation of a dye.

4.2. Dissipative Self-Assembly

Carbodiimide chemistry—introduced in section 3.1—is often employed in the context of non-equilibrium self-assembly, sometimes referred to as dissipative self-assembly.^[104] In systems associated to this domain, an agent usually referred to as fuel^[104,105] (e.g., a template, an electron, light, or a coupling agent) promotes the formation of a species that can self-assemble, but this species is thermodynamically unstable under the experimental conditions, requiring a continuous fuel supply to persist.

Numerous examples of such systems have been reported to date.^[61,63,106,107] When considering these systems in relation to ratchet mechanisms, different levels of complexity can be found. At one extreme, no ratchet mechanism is active and no endergonic reaction takes place. At the opposite extreme, the experimental observations imply a level of complexity that is higher than the one of ratchet mechanisms covered in this review. For example, bistability and oscillations have both been realized experimentally.^[108–111] These effects require an underlying chemical reaction network that is topologically more complex^[112] than those presented here: the ratchet framework might be too simplistic to describe these phenomena, but the observations imply the occurrence of endergonic reactions. In the following, we discuss some aspects of non-equilibrium self-assembly relevant to ratchet mechanisms.

In the simplest case, we consider the assembly of surfactant **28** into vesicles, templated by ATP (Figure 15a).^[113] In the presence of an enzyme that degrades ATP into the corresponding monophosphate (AMP) and inorganic phosphate, the templated structure becomes transient. At any moment of the transient process, all reactions of the system evolve toward thermodynamic equilibrium, and never against it. Thus, no endergonic reaction takes place: we can identify a driving reaction, but it's not possible to identify a driven one. A driven reaction capable of absorbing energy should be part of a reaction

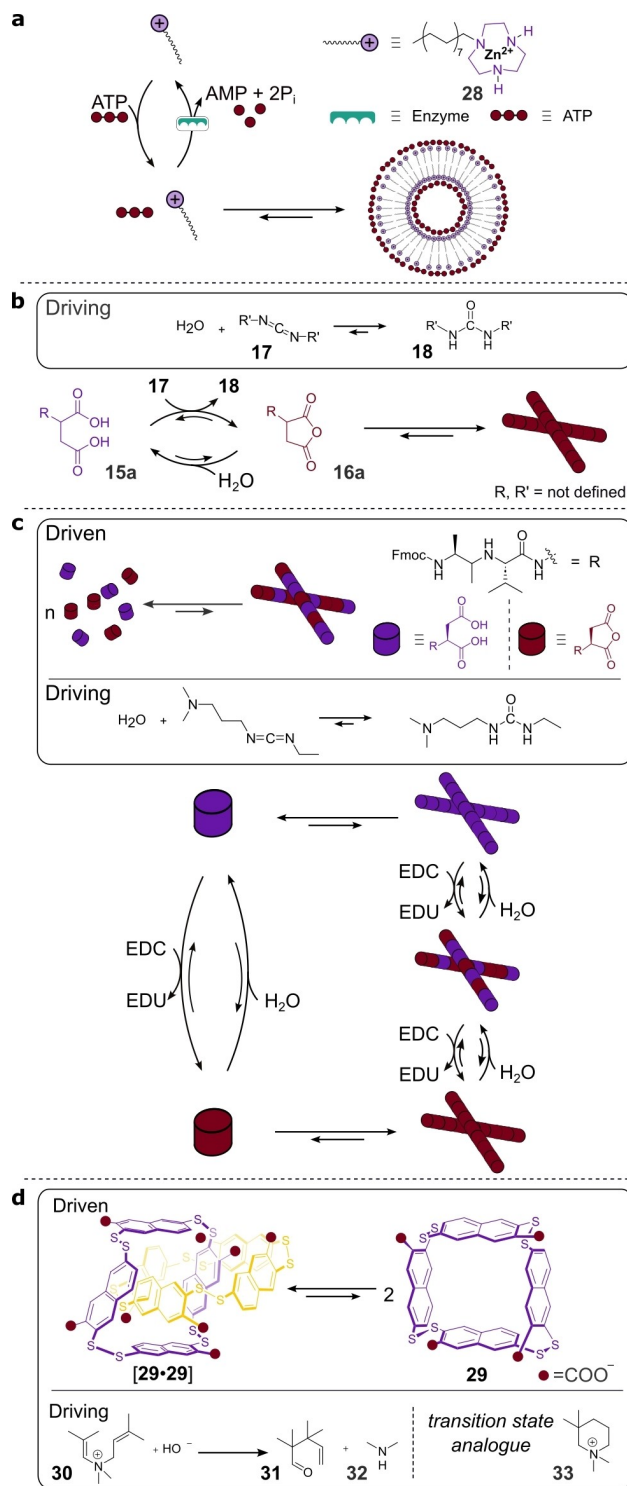


Figure 15. Reaction networks describing: a) the transient assembly of vesicles templated by ATP; b) a transient assembly powered by carbodiimide hydration; c) the chemically-driven assembly of fibers powered by carbodiimide hydration. d) Dynamic covalent reaction that can be shifted towards the formation of dynamic covalent macrocycles in the presence of transition state analogues. EDC = 1-ethyl-3-(3-dimethylaminopropyl)carbodiimide; EDU = 1-ethyl-3-(3-dimethylaminopropyl)urea.

cycle associated with the conversion of ATP into AMP and P_i , and there should be a sequence of steps that corresponds to the sum of driven and driving reaction, as we have seen in sections 2 and 3. Here, the self-assembly reaction is off-cycle and no ratchet can arise.

We can imagine a similar system in which the formation of a species prone to self-assembly is induced by the formation of an anhydride, promoted by carbodiimide (Figure 15b). In line with the discussion on carbodiimide chemistry in section 3.1, the network includes a ratchet mechanism (associated with carbodiimide hydration, Figure 8a). Still, the self-assembly reaction remains off-cycle, and therefore the self-assembly reaction would simply adjust to the concentration of anhydride. Drawing a parallel with rotary motor **19**, such a system would have only one of the two ratchet mechanisms.

If we now consider that anhydride formation and hydrolysis can occur also in the fibers, we recover a square reaction network (Figure 15c). This situation maps more closely the experimental evidence obtained on peptide Fmoc-AVD and its analogues (A is alanine, V is valine, and D is aspartic acid, Figure 15c).^[114] It was shown that both anhydride formation and hydrolysis can take place in the fibers, and in these fibers their rate is accelerated. These observations point at presence of information ratchet effects. Differences in the speed of activation and deactivation between the assembled and disassembled states have been observed in multiple other systems.^[110,114–118] However, further studies are desirable to explore how such differences can impart emergent properties.

The reaction network in Figure 15c is closely related to the one in Figure 9, used to describe the principles of information ratchets. In this case the horizontal reactions correspond to self-assembly steps. How information ratchet effects can arise in such a network is tightly related to the discussion presented in section 3.2, and was previously illustrated by us and others; thus we refer readers to previous works for the details.^[45,76,119,120] Prominent examples of non-equilibrium self-assembly, such as microtubules and actin, seem to include an information ratchet mechanism, which encourages further studies on kinetically asymmetric artificial fibers.^[45,120]

An additional element to consider is how carbodiimide is supplied. The illustrated systems can be operated with batch-exursion experiments or through continuous addition. In contrast, the theory of chemical reaction networks considers system dynamics once the concentration of carbodiimide is kept constant (chemostatted), a condition rarely realized experimentally.^[121,122] As a result, there is often a discrepancy between theoretical frameworks and experimental reality.

A situation in which this discrepancy becomes particularly relevant involves energy ratchet mechanisms. Indeed, as discussed in sections 2 and 3, energy ratchet powered by chemical reactions requires alternating environmental conditions. Therefore, under stationary conditions this kind of energy ratchet cannot operate. In contrast, during batch experiments the concentration of carbodiimide is high at the beginning and gets lower as it is consumed. This experimen-

tal routine is conceptually equivalent to alternating high and low concentrations of carbodiimide, which can enable the operation of energy ratchet mechanisms (section 2). Reconsidering literature data in light of this, kinetic trapping of fibers at the end of a batch excursion experiment—which is frequently observed—is consistent with the operation of an energy ratchet mechanism.^[59] Moreover, repeated additions of carbodiimide could also lead to the self-selection of anhydrides more stable under hydrolytic conditions, which is a non-equilibrium effect.^[115]

To summarize, in batch excursion experiments powered by carbodiimide hydration on dissipative self-assembling systems, we can identify at least four ideal cases: 1) no ratchet mechanism active at all, besides the well-established carbodiimide chemistry itself; 2) an information ratchet, due to kinetic asymmetry; 3) an energy ratchet associated with a change in carbodiimide concentration; 4) emergent effects that cannot arise in minimal chemical reaction networks, such as bistability.^[110]

On top of the challenges posed by non-equilibrium conditions, the typical difficulties posed by supramolecular assemblies (polymers, vesicles, micelles, etc.) remain. For example, it is not possible to precisely identify all the species involved, and rationalizations need to rely on simplified models that may overlook important factors. It is well known in supramolecular chemistry that seemingly irrelevant details can be the source of emerging phenomena.^[123] Therefore, when dealing with large assemblies, it seems almost hopeless to map the observed behavior to minimal chemical reaction networks, using the same level of detail currently applied to molecularly defined systems. Recent advances in the field have illustrated that this challenging aspect is not hampering progress. Experimental evidence and observed properties have a central role.

Dynamic covalent libraries often have the advantage that the assembled structures are precisely defined.^[124] The Otto group has extensively investigated dynamic covalent libraries. In a significant example, they studied a library comprising catenane **[29·29]**.^[125] When exposed to substrate **30**, the library modified its composition, shifting to macrocycle **29** (Figure 15d). This substrate can undergo Aza-Cope rearrangement to **31** and **32**, catalyzed by the library. Based on the published information it is not possible to discuss in detail the kinetic asymmetry of that network. However, the experimental evidence points at the presence of a ratchet mechanism, because part of the energy provided by the catalyzed reaction is absorbed to form high-energy tetramers that revert to thermodynamically stable catenanes with a kinetic that is somewhat slower than the catalyzed rearrangements. In this case, both an energy and/or an information ratchet mechanism might be active. The authors gained insights into their system using a transition state analog **33**, which shifted (thermodynamically) the dynamic library composition. The same approach might be extended to other systems, facilitating the design of endergonic reactions.

5. Energetic Considerations

As steam engines inspired 19th Century physicists to develop classical thermodynamics, molecular ratchets are now challenging our understanding of how energy and information are processed at small scales. In the following we describe the energetic contributions that can be considered to analyze energy absorption by a molecular ratchet mechanism.

5.1. Stored Energy

The ratchet mechanisms considered so far use energy to generate non-equilibrium species concentrations. How much free energy is stored in a non-equilibrium distribution is well established.^[126] Each species *i* contributes to the stored free energy based on how much its concentration moves away from its equilibrium value. As a result, the stored energy can be expressed using the concentration of each species at equilibrium ($[i]_{\text{eq}}$) and in the non-equilibrium state ($[i]$) as in equation 8. The total free energy stored is then the sum of each species' contributions:

$$\text{stored free energy} = RT \sum_i \left([i] \ln \frac{[i]}{[i]_{\text{eq}}} - [i] + [i]_{\text{eq}} \right) \quad (8)$$

Equation 8 is expressed in units of energy per volume. In some cases, it might be insightful to normalize the value of the stored free energy for the total concentration of species such to express it in units of energy per mole. However, when a system comprises bimolecular reactions such as self-assembly steps, the total concentration may vary, making the choice of the normalizing concentration somewhat arbitrary.

The physical meaning of equation 8 is that the calculated stored free energy is the energy released when the system relaxes to the equilibrium state. All reactions of the network can contribute to this energy. For example, in molecular ratchets based on photoswitches, free energy is stored both by populating the thermodynamically less stable isomers of photoswitches (dark green in Figure 16a) and by shifting the driven reaction (light green in Figure 16a). The strategies to recover (and use) the energy stored by these distinct reactions might be very different. Thus, to quantify the efficiency in a practically meaningful way, in some cases it is reasonable to focus only on one of the two types. A possibility is to consider only the energy stored in the driven reaction. This strategy was applied to quantify the free energy stored in experimental systems. In particular, a second-generation light-driven pump based on **25** (Figure 12) stored 0.63 JL^{-1} ,^[127] chemically driven rotaxanes in which ring position was altered stored $3.0\text{--}4.3 \text{ JL}^{-1}$,^[128] and a hydrazone formed thanks to an energy ratchet mechanism (section 2.1) stored 0.49 JL^{-1} .^[24] Considering that species population was obtained from NMR data in all these cases, the similarity between these values becomes less surprising. At present most studies in this area rely on NMR data, and this fact poses some experimental limitations to the concentration ranges that can be explored. Calorimetry experi-

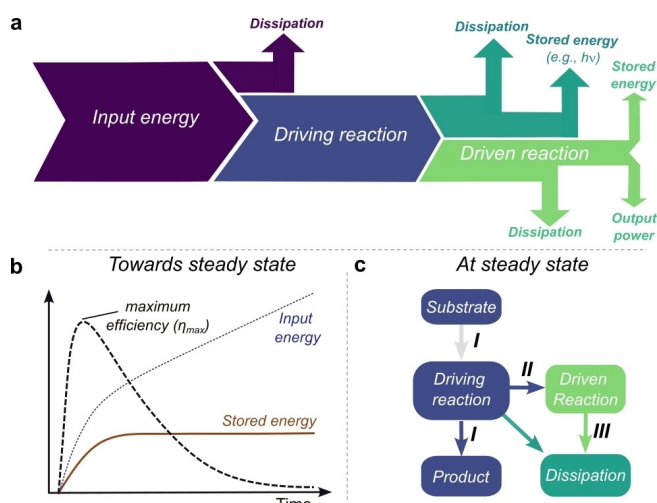


Figure 16. a) Sub-sets of amounts of energy to consider when calculating the thermodynamic efficiency of a molecular ratchet mechanism; b) evolution of input power, stored energy and efficiency while reaching and maintaining the steady-state; c) key energy consumption processes at the steady state for a chemically-driven system.

ments performed on a pseudorotaxane (see below, [35C34] in Figure 18a) gave direct access to the enthalpic contribute of the stored energy in that system, affording a value of 70 JL^{-1} when the system is operated at 5 mM, the conditions used in that work for NMR studies.^[129]

5.2. Input Energy

To understand how efficient molecular ratchets are, we need to identify how much energy is provided to realize the target endergonic process. Some of the input energy is lost in unproductive ways, even regardless of the interplay with the driven reaction (Figure 16a). Therefore, depending on the energy source, multiple reasonable choices are possible to identify the relevant input energy.

When considering chemically-driven systems, often there is a background reaction, such as $S \rightarrow P$ or other unwanted decomposition reactions. Only a fraction of *S* interacts with the operating system; e.g., Fmoc derivative **12** in Figure 7 suffers from a decomposition process simultaneous to its reaction with dumbbell **11**. Considering all the free energy released by *S* conversion, regardless of whether the operating system catalyzes it, gives a correct estimate of the energetic cost of operating the ratchet mechanism. However, accounting for the background decomposition of *S* in the input free energy leads to values that can be largely unrelated to ratchet operation, and reflect substrate's stability, presence of competitive species, or even the volume in the case of heterogeneous systems. Therefore, to assess ratchets' performance, at present it might be more insightful to solely consider the fraction of *S* converted into *P* by the molecular ratchet.

In electrochemical systems operated in a bipotentiostatic configuration (Figure 6), in addition to the current flowing between the working electrodes—responsible for the ratchet operation—another current will flow between the working electrodes and the counter electrode. The magnitude of this unproductive current is highly dependent on specific features of working electrodes (dimension, position, etc.). This current may even be orders of magnitude larger than the productive one. If such a contribution is considered, it prevents assessing electrically driven systems' performance. Considering the state-of-the-art, it might be insightful to solely consider the current flowing between the two working electrodes, in analogy to neglecting the background substrate decomposition in chemically-driven systems.

When dealing with light-driven systems involving photo-switches, we can consider the following contributions: 1) the photons emitted by the light source; 2) the photons incident on the sample; 3) the photons absorbed by the sample; 4) the photons that induced a photoisomerization event. When calculating the thermodynamic efficiency of a ratchet mechanism, any of these amounts of photons—thus free energy^[41]—could be employed. To evaluate the ability of the molecules to harvest free energy from the light, it might be more insightful to consider the photons absorbed by the sample, as the first two quantities strongly depend on the experimental setup, rather than molecular properties.

Overall, the outlined choices share the fact that only the fraction of energy consumed via an interaction with the ratchet's components is considered. This approach has two benefits. The first is that it gives a quantitative measure of the ratchet performance from an energetic viewpoint, complementary to kinetic quantities like kinetic asymmetry. The second advantage is that it allows for more meaningful comparisons between ratchet systems powered by different energy sources or operated in different conditions. Considering all the free energy that gets consumed while the ratchet is operated is key for any practical application, but it seems premature to consider.

5.3. Thermodynamic Efficiency

Most artificial systems are not able to further exploit the absorbed energy, driving other processes away from equilibrium (no output power in the scheme of Figure 16a); therefore, the current focus is on the efficiency of energy storage. The latter is computed as a ratio between the energy stored by the system and the input energy, discussed in the two latest sections.^[119] To calculate the efficiency of an energy ratchet such as the pseudorotaxane in Figure 2, one could switch the redox environment back and forth one time, calculating the stored energy using equation 8, and the ΔG of the driving reaction as input energy. If multiple redox alternations are done to drive the system progressively away from equilibrium, the ΔG of the driving reaction needs to be multiplied by the number of alternations performed.

The situation is less straightforward when considering autonomous ratchets, because after some time the system reaches a steady state: the concentrations of species are

stationary, thus the stored energy remains constant, but the input energy keeps increasing. As a result, the efficiency increases at the beginning (when the concentrations depart from equilibrium), reaches a maximum, and then decreases over time, tending to zero (Figure 16b). To compare different systems on the same ground, a possibility is to compare the efficiency at peak.^[119] An alternative is considering the input free energy needed to reach the steady state. While viable, these strategies are rarely used to calculate the efficiency of autonomous artificial systems.

The strategy more frequently used to calculate the efficiency of autonomous ratchets is based on the properties of the steady state. In fact, the formalism is rooted in the study of biomolecular machines, which are multicomponent systems. This peculiarity led scientists to evaluate the efficiency at which free energy flows between the different components involved in energy transduction, at the steady state.^[130] The same approach is now commonly used to define the thermodynamic efficiency for a ratchet mechanism operating at the steady state, even if it does not perform any measurable work.^[49,119,127,131,132]

Instead of the energy, the focus is on the power. The input power is the amount of free energy consumed by the ratchet mechanism in a time unit, e.g., the speed at which substrate is consumed multiplied by the ΔG associated with $S \rightarrow P$ reaction (**I** in Figure 16c). At the steady-state, each reaction dissipates a certain amount of power, and this approach considers the power dissipated by the reactions that are driven away from equilibrium. For example, for the driven reaction $L \rightleftharpoons H$ alone, one would consider the power dissipated at the steady-state by this particular reaction (**III** in Figure 16c) which is:

$$\text{dissipated power}_{L \rightleftharpoons H} = RT(\ln K - \ln Q)(k_+[L] - k_-[H]) \quad (9)$$

The first term in parenthesis contains the reaction quotient Q and reports on how far the reaction is from equilibrium. The second term in parenthesis is the net speed of $L \rightleftharpoons H$ reaction. Intuitively, fast reactions that are far from equilibrium dissipate a lot. However, since we are considering a steady-state, at least the same amount of dissipated energy must be absorbed from the input energy in a given time interval (component **II** in Figure 16c). For this reason, we can use the dissipated energy to calculate the efficiency. If other reactions are driven against the thermodynamic potential—e.g., $L' \rightleftharpoons H'$ —their contribute should also be added.

Considering the systems for which this approach has been applied, it emerges that the efficiencies are usually very low, such as $10^{-6}\%$ for a chemically-driven catenane rotary motor, and 10^{-1} – $10^{-2}\%$ for light-driven pumps.^[69,127,131] One reason for this is that both systems exploit highly energetic sources, in the order of $100 RT$. This value is significantly higher than those found in nature, for example a ΔG of $26 RT$ was found for ATP hydrolysis in human muscle cells at rest.^[133] In this regard, using electrical energy seems advantageous, as it allows for modulating the energy supply. Possibly also for this reason, the autonomous self-assembling system presented in section 2.5 is the most

efficient system reported to date, with a 9% efficiency obtained when subject to a driving energy of 31 RT , closer to what is found in biology.

5.4. The Broader Context: Carnot, Onsager, and Prigogine

One celebrated result from classical thermodynamics is that the efficiency of a machine powered by a temperature difference ($T_{\text{high}} - T_{\text{low}} > 0$) is limited by Carnot's cycle efficiency ($1 - T_{\text{low}}/T_{\text{high}}$), i.e., the most efficient thermodynamic cycle working between two thermal reservoirs.^[134] In general, this result does not apply to chemical systems, as they are typically not powered by temperature differences, being in contact with a single thermal reservoir (the solution). This means that, in theory, there are no intrinsic limitations other than the second law of thermodynamics (efficiency should not exceed one) to the efficiency of ratchet mechanisms.

In principle, an exception is represented by photochemical systems powered by light bulbs generating light via incandescence (e.g., tungsten incandescent lamps). In these cases, the radiation emitted by the lamp originates from having heated the bulb. Therefore, the source of energy is again a thermal difference. Formally, the light source can be treated as a thermal reservoir characterized by the temperature of the bulb, and Carnot's bound is therefore recovered.^[41,127]

The works of Onsager and Prigogine are milestones of chemical non-equilibrium systems. They both discussed how non-equilibrium systems respond as the thermodynamic driving force increases—here, the ΔG associated to $S \rightarrow P$ reaction. If we consider a kinetically asymmetric system and imagine beginning from $\Delta G = 0$ (equilibrium) and then slightly increasing the ΔG to bring the system away from equilibrium, the cyclic chemical current will initially change linearly proportional to the ΔG .^[134] This is the so-called “linear regime”. Special theorems hold in the linear regime, including a series of results that constraint the efficiency to be maximized in the equilibrium limit (very small forces and/or very slow driving process) where the output power goes to zero (practically useless limit).^[134]

A peculiarity of chemical systems is that under typical experimental conditions they commonly operate beyond the “linear regime”, making it possible to optimize efficiency and power at the same time.^[119,135] Not obeying linear regime assumptions is necessary to obtain complex dynamic behaviors such as negative differential response,^[136] pattern formation,^[137] and oscillations.^[138] Whether these emerging phenomena can be observed depends on the specific structure of the network. For example, square schemes are already sufficient to have a negative differential response (a bigger ΔG leading to a smaller current). On the other hand, no matter how large the ΔG , square schemes cannot afford oscillations and patterns, which Prigogine referred to as “dissipative structures”. When emergent phenomena are observed, there has to be a more complex mechanism in action.

6. Ratchets in Other Domains

6.1. Bioenergetics

Ratchet mechanisms are exploited by living organisms, so it is spontaneous to wonder their role in the origin of life, be it in a prebiotic context or *de novo*. Energy ratchets are brought about by changes in environmental conditions, which happen commonly. Physical non-equilibria in a prebiotic context have been recently discussed by Braun et al.^[139] We can distill the different outlined scenarios into spatial separation, alternating conditions (temperature,^[140] pH, salt concentration, etc.) and photochemical reactions. As a matter of fact, all these cases could be described within the ratchet framework. Moreover, we presented in section 3.1 how activation chemistry is part of ratchet mechanisms, and it has also been employed in a prebiotic context. In particular, repeated acylations of glycerol phosphate under hydrolytic conditions were exploited to accumulate acylglycerol phosphates.^[141] These phosphates could accumulate because they self-assembled into vesicles featuring slower hydrolysis, resulting in kinetic schemes that share some analogies with previous examples of energy ratchets progressively driven away from equilibrium.

In contrast to energy ratchet mechanisms, information ratchet mechanisms are harder to envision in a prebiotic setting. One particular case of information ratchet is the sequence-dependent photodamage of nucleic acid sequences.^[139] However, modern biology exploits chemically-driven information ratchets extensively, rather than light-driven ones. Several types of molecules have been discussed as energy sources powering ancient metabolism, including metals, O_2 , hydrogen peroxide, thioesters and phosphate derivatives.^[142–145] However, detailed energy transduction mechanisms operating at the steady-state remain elusive, although the role of preferential pathways has been recognized.^[146] The ratchet mechanisms framework can contribute by pointing to the features of chemical reaction networks required for energy transduction. Such features are largely independent of the type of molecules involved, and encompass the role of compartmentalization.^[147,148] Thus, ratchets would be consistent with the current understanding of free-energy transduction in metabolic networks.^[149]

Considering kinetically asymmetric networks, redox equilibria seem strong candidates for the emergence of information ratchet mechanisms. Taking O_2 as an example, this simple molecule has a high energy content—being considered the terminal electron acceptor^[150]—while it gets reduced slowly, requiring catalysts in the majority of cases. As a result, even simple metals capable of catalysing O_2 reduction might satisfy the requirement needed to realize energy transduction processes by leveraging constant energy sources.^[145,150–152]

As it would be in the case of O_2 reduction, any ratchet mechanism based on chemical catalysis relies on substrates that are thermodynamically activated, but kinetically stable. These features are shared by several molecules that power cell metabolism, including ATP and related nucleoside

triphosphates, nicotinamide adenine dinucleotides, acetyl coenzyme A, *S*-adenosyl methionine, carbamoyl phosphate, uridine-diphosphoglucose, and isopentenyl diphosphate.^[151] Apart from O₂, all these molecules have the potential to transfer a functional group. This observation rooted in biology points at the relevance of group transfer in non-equilibrium systems even besides biology. So far, only a few artificial molecular ratchets rely on group transfer, one of them being rotaxane [11C10] (Figure 7). In that case, incorporation of Fmoc group in the dumbbell blocks the self-assembly equilibrium which enables accumulating high-energy [11C10]. This example illustrates that while we should be able to identify clearly a driving and a driven reaction, the two reactions might also have some components in common, as occurring in some biological examples, e.g., in microtubules.^[153]

6.2. Proofreading

A biological process that can be realized via energy or information ratchet mechanism is error correction, the process by which high chemoselectivity is achieved, also referred to as proofreading. This process is particularly important in relation to nucleic acid sequence replication. Naturally occurring RNA presents exclusively 3',5'-phosphodiester bonds, and not 2',5'-bonds, so in a prebiotic context it is relevant to understand how 3',5' linkages could be accumulated. Several possibilities have been explored theoretically.^[154,155] A possibility that has been experimentally explored relies on subsequent steps of acetylation, ligation, and hydrolysis (Figure 17a).^[156] Cleavage of 2',5'-phosphodiester bonds leads to a 2',3'-cyclic phosphate that further rearranges to a 3'-monophosphate. Under acetylating conditions, the monophosphate is acetylated at its 2' position, preventing the participation of the 2'-oxygen in subsequent ligation reactions promoted by phosphate activating agents. Formation of 3',5'-phosphodiester bond is followed by acetate hydrolysis, affording the overall conversion of a 2',5'-bond into a 3',5'-bond, which is accumulated because its hydrolysis is slower in comparison to that of 2',5'-phosphodiester bond. Related strategies employing

activated nucleotides have been used to recover RNA replication ability.^[157]

While alternating environmental conditions can afford error correction mechanisms, modern biology relies on enzymatic kinetic proofreading, which relies on differences in transition states.^[154,158] Different models have been proposed, and they all contain a driven step: a key proofreading element that is often treated implicitly, but can be made explicit by implementing an information ratchet mechanism. To illustrate it, we revisit the Hopfield model^[158] as follows. We consider the formation of a dimeric species (M₂, two green dots) via a sequence of steps involving enzyme E (Figure 17b). It is also possible that the wrong monomer (red dot) enters the catalytic cycle; in this case, it is desirable that the ternary complex [E·M·M] reverts to the initial state, instead of proceeding to form the unwanted dimer. Usually, the thermodynamic stability of the ternary complex is similar regardless of the monomer included (right or wrong), and kinetic features are key to select which path prevails once the ternary complex is formed. In the absence of a ratcheting cycle involving the conversion of S into P, the ternary complex disassembly (desirable in the presence of the wrong monomer) closes a reaction cycle. Therefore, the microscopic reversibility constraints presented in section 3.2 require that a fast disassembly of the ternary complex must be accompanied by its concomitant fast assembly, which is undesirable. Information ratchet mechanisms come to the rescue: if the assembly of [E·M·M] is driven by a ratchet mechanism, the population of the ternary complex is disentangled from microscopic reversibility, allowing to have a fast disassembly reaction once the wrong monomer is incorporated.

Overall, including an information ratchet has two advantages: it enables the synthesis of molecules in conditions in which they are thermodynamically disfavored, and allows to achieve higher precision in the synthesis of sequence-defined polymers. Related kinetic schemes can involve the disassembly of the product, instead of intermediate complexes,^[154] and this framework has also been validated experimentally using polymerase chain reaction.^[159] Finally, spatial differentiation coupled with

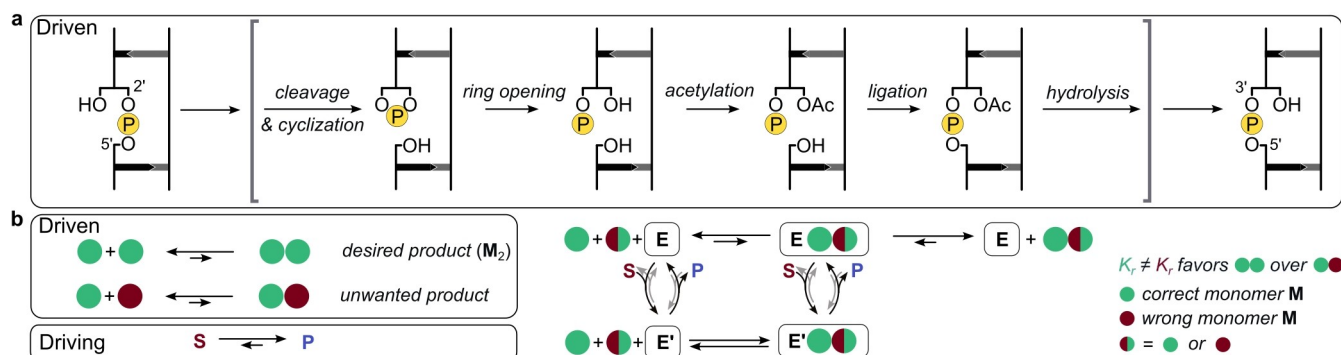


Figure 17. a) Reaction sequence associated with non-enzymatic proofreading under prebiotic conditions; b) reaction network associated with forming high-energy homodimer M₂, thanks to an enzymatic proofreading step.

diffusion has also been proposed as underlying proofreading mechanisms.^[160]

6.3. Technology

What new technologies may emerge from the implementation of ratchet mechanisms? The field of molecular machines has attempted to address this question,^[161] for example by realizing responsive materials that can absorb and release energy, or store information.^[162–164] Implementing molecular ratchets seems a viable route to transition from responsive to adaptive materials, and install life-like properties.^[165,166] However, real-world applications remain elusive.

Detaching from directional motion and focusing on obtaining high-energy structures opens new possibilities, for example related to cooling technology.^[167] Indeed, ratchet mechanisms can enable the formation of ordered structures, characterized by negative ΔS of formation. As a result, relaxation of the high-energy state to equilibrium might be driven by a positive ΔS and being associated with a positive ΔH , which implies cooling down the surrounding, as heat is absorbed in the relaxation reaction. We have contributed to explore this direction by investigating the energetic content of a high-energy pseudorotaxane composed of macrocycle **34** and dumbbell **35** (Figure 18a).^[129] The high-energy state is formed via an energy ratchet mechanism powered by an acid-base reaction, which results in a crown-ether residing onto a triazolium station. Relaxation from the high-energy

state to equilibrium is an endothermic reaction having a ΔH of 20 kJ/mol, and it seems reasonable to expect similar enthalpies for related high-energy structures that inspired our study.^[27,164,168] The amount of heat absorbed is comparable with the one of ammonium chloride dissolution in water, commonly used in instantaneous ice packages.^[169] Powering similar systems with electricity is within reach, and would lead to recyclable instant cold packages.

The conversion of electrical voltages into temperature differences and vice versa are known as thermoelectric effects. Recently, it was shown that redox-active systems can boost such effects. In particular, a mixture of α -cyclodextrin and I^3^- afforded a Seebeck coefficient of 1.97 mV K^{-1} , which is higher than conventional thermoelectric materials.^[170] Therefore, applying ratchet mechanisms to advance heating/cooling technologies may be within reach. These examples may seem of limited impact at first, but the market of such technologies has an estimated value of one billion dollar, highlighting how seemingly tangential applications may have significant impact.

At a more general level, we note that energy ratchet mechanisms rely on fluctuating environments. Therefore, they may help to design systems that harvest energy from small fluctuations. Such devices have a huge potential for the realization of sustainable technology. An example is offered by a macroscopic actuator based on a carbon nitride polymer (Figure 18b).^[171] This actuator responds to the adsorption and desorption of water associated with fluctuations in ambient humidity, resulting in a seemingly autonomous macroscopic motion. Studies like this one and others also point to the importance of macroscopic geometrical constraints when realizing actuators based on chemical processes.^[172,173] This factor becomes even more crucial when considering light-driven actuators.^[173–177]

A feature common across different ratchet mechanisms is that an effective ratchet offers a fast route for the occurrence of the driving reaction. In other words, the fastest reaction path for the driving reaction is the one coupled to the driven reaction. Therefore, it is possible to look at ratchet mechanisms as catalytic networks for the driving reaction. In this framework, developing efficient catalysts and ratchet mechanisms are overlapping areas of science. For the moment, the possibility of alternating conditions to promote catalytic processes beyond the Sabatier limit has been discussed mostly at the computational level and for heterogeneous catalysis.^[178] Yet, the potential of these technologies is huge: even ammonia synthesis would be accelerated by applying a dynamic strain to a Ru-based heterogeneous catalyst.^[179] Generating power from below-band gap excitation in semiconductors has also been framed in this context.^[180] Examples of technologically relevant reactions that benefit from alternating environments have been reported, often in relation to electrochemical processes: these systems might leverage energy ratchet mechanisms, albeit not framed in this context.^[181–183]

The role of autonomous ratchets in improving catalytic abilities is largely unexplored, albeit intrinsic to their operation mechanism, particularly when the substrate-binding reaction is favored in one state, and the product-

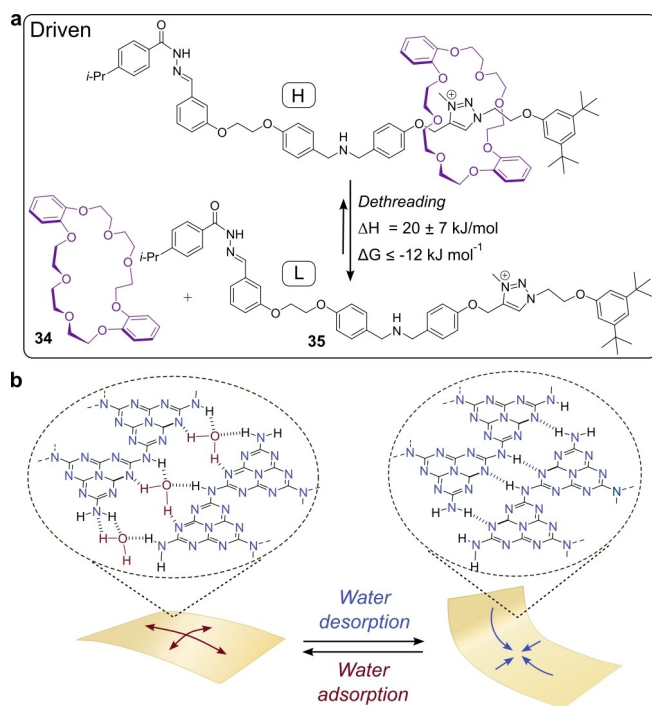


Figure 18. a) Endergonic reaction powered by acid-base reactions which affords a low-entropy state which cools down the surroundings when relaxing to equilibrium; b) representation of an autonomous actuator powered by small fluctuations in ambient humidity.

releasing reaction in the other one, i.e., doubly gated.^[57] In small-molecule catalysts, these effects arising from catalyst dynamics did not receive much attention from the community, while almost certainly taking place. On the contrary, the role of conformational dynamics is gaining more attention, being discussed more frequently in biological enzymes.^[184,185] Making more efficient catalysts by engineering catalyst conformational dynamics is a direction to which ratchets can contribute.

7. Summary and Outlook

In this tutorial review, we have presented artificial molecular ratchet mechanisms, by focusing on the features of the chemical reaction networks from the perspective of mass-action kinetics. This choice allows describing chemically-, light-, and redox-driven systems in a coherent way, and highlights overarching principles common to different systems and energy sources. We grounded our discussion in the self-assembly of pseudorotaxanes—developed in the context of molecular machines—while highlighting connections with other fields. In particular, we discussed in greater detail the connection with bioenergetics and prebiotic chemistry, as well as non-equilibrium self-assembling systems, since we are confident that scientists operating in these areas might find the ratchet framework a useful rationalization tool, fostering progress.

The outlined ratchet mechanisms are very general. Indeed, the reaction networks highlighted in this review are among the simplest that can give rise to endergonic reactions. In this regard, the difference between having or not having a ratchet mechanism active marks the ability of the system to absorb energy from the environment. This ability is a sharp thermodynamic boundary, representing an essential prerequisite to developing systems that are not merely responsive (switches) but are adaptive, i.e., having a memory of the past and thus responding differently upon subsequent stimuli.^[165,166] However, the described ratchet mechanisms are insufficient to describe every known non-equilibrium phenomenon. Therefore, it is important to highlight some limitations of the networks presented herein, which offer opportunities to develop the understanding of endergonic reactions further.

The most relevant aspect that has not been treated is likely feedback mechanisms. Here we intend feedback as a process by which a system is regulated by its output.^[186] An example is when a product of a given reaction acts as a catalyst for another reaction. Autocatalysis, replication, and negative feedback are all phenomena that are related to feedback mechanisms. They cannot emerge in chemical reaction networks as simple as those discussed in this review, while being essentials for designing adaptive systems displaying behaviors reminiscent of intelligence.^[162,165,166] Still, experiments continue to teach chemists that reality is more complex than our rationalizations, and even very simple molecules can hide more complicated networks—having feedback mechanisms. For example, when a dumbbell as simple as 2^{3+} bears a glycol collecting chain instead of an

alkyl one, the dethreading reaction becomes autocatalytic.^[16] Considering how much complexity can be hidden in a simple dethreading reaction, where large supramolecular assemblies are investigated, kinetic schemes can only serve as a rough guide. Yet, they are useful even when seeking emergent phenomena, such as oscillations.^[187]

Diffusion and spatial phenomena are not much explored in relation to ratchet mechanisms. Here we have covered examples where a detailed analysis was available, but active transport and the formation of spatial gradients have also been reported.^[9] Geometrical aspects are also key when considering redox-driven systems powered by heterogeneous electron transfer,^[20] and light-driven systems. For example, carefully selecting the irradiation geometry can give rise to emergent nonlinear dynamics such as bistability and oscillations.^[188] Oscillating systems are complex, and examples of chemically-driven oscillating systems displaying self-assembly have been realized only recently, powered by redox reactions.^[108,111] Since chemically-driven oscillations can emerge under constant environmental conditions, information ratchets may be involved, while less likely energy ratchets. Albeit a conceptual connection between information ratchets and oscillations has been made,^[189] a clear mathematical relation—if at all present—still remains to be disclosed.

Biological complexity features a combination of network complexity (e.g., feedback loops), compartmentalization, and exposure to alternating conditions (e.g., light and dark). It appears that high-throughput experimentation, combined with data science and machine learning methods are facilitating the transition of some model systems into what could be considered topics of *tractable complexity*.^[190] For example, insights into the formose reaction have been recently obtained, and exposure to dynamic conditions such as varying $\text{Ca}(\text{OH})_2$ concentration in time affects system's composition.^[191] Such an observation could be consistent with the operation of an underlying ratchet mechanism.

Overall, ratchet mechanisms are emerging as a chemistry crossroad, underlying several scientific grand challenges^[2] and hallmarks of life.^[192] As a result, discussions on terminology have appeared,^[193] but thermodynamics comes to the rescue in many cases, as there is a clear demarcation line between exergonic and endergonic reactions. When a detailed description of system's thermodynamics is difficult to access, focusing on the novelty of the experimental observations rather than the underlying principles can be a solution. Bringing together expertise from multiple areas of science via the endergonic reactions crossroad, and implementing ratchet mechanisms besides molecular machines to realize a multitude of endergonic processes, will lead to major breakthroughs in areas key to our society.

Acknowledgements

This work was supported by the Interdisciplinary Thematic Institute ITI-CSC via the IdEx Unistra (ANR-10-IDEX-0002) within the program Investissement d'Avenir and the European Research Council (ERC-2021-StG n. 101041933).

The authors would like to thank warmly Dr. Shuntaro Amano, Prof. Dean Astumian, Prof. Job Boekhoven, Dr. Claudia Bonfio, Prof. Joseph Moran, and Prof. Simone Pigolotti for constructive feedback.

Conflict of Interest

The authors declare no conflict of interest.

Data Availability Statement

Data sharing is not applicable to this article as no new data were created or analyzed in this study.

Keywords: Catalysis · Molecular Machines · Non-Equilibrium Systems · Photoswitches · Systems Chemistry

- [1] B. A. Grzybowski, W. T. S. Huck, *Nat. Nanotechnol.* **2016**, *11*, 585–592.
- [2] G. M. Whitesides, *Angew. Chem. Int. Ed.* **2015**, *54*, 3196–3209.
- [3] R. D. Astumian, *Science* **1997**, *276*, 917–922.
- [4] C. S. Peskin, G. M. Odell, G. F. Oster, *Biophys. J.* **1993**, *65*, 316–324.
- [5] C. J. O. Reichhardt, C. Reichhardt, *Annu. Rev. Condens. Matter Phys.* **2017**, *8*, 51–75.
- [6] B. Lau, O. Kedem, J. Schwabacher, D. Kwasnieski, E. A. Weiss, *Mater. Horiz.* **2017**, *4*, 310–318.
- [7] E. R. Kay, D. Leigh, F. Zerbetto, *Angew. Chem. Int. Ed.* **2007**, *46*, 72–191.
- [8] F. Jülicher, A. Ajdari, J. Prost, *Rev. Mod. Phys.* **1997**, *69*, 1269–1281.
- [9] S. Erbas-Cakmak, D. A. Leigh, C. T. McTernan, A. L. Nussbaumer, *Chem. Rev.* **2015**, *115*, 10081–10206.
- [10] S. Kassem, T. Van Leeuwen, A. S. Lubbe, M. R. Wilson, B. L. Feringa, D. A. Leigh, *Chem. Soc. Rev.* **2017**, *46*, 2592–2621.
- [11] M. Baroncini, S. Silvi, A. Credi, *Chem. Rev.* **2020**, *120*, 200–268.
- [12] R. D. Astumian, *Biophys. J.* **2010**, *98*, 2401–2409.
- [13] A. I. Brown, D. A. Sivak, *Chem. Rev.* **2020**, *120*, 434–459.
- [14] M. L. Mugnai, C. Hyeon, M. Hinczewski, D. Thirumalai, *Rev. Mod. Phys.* **2020**, *92*, 25001.
- [15] E. Branscomb, T. Biancalani, N. Goldenfeld, M. Russell, *Phys. Rep.* **2017**, *677*, 1–60.
- [16] C. Cheng, P. R. McGonigal, W. G. Liu, H. Li, N. A. Vermeulen, C. Ke, M. Frascioni, C. L. Stern, W. A. Goddard, J. F. Stoddart, *J. Am. Chem. Soc.* **2014**, *136*, 14702–14705.
- [17] H. Li, C. Cheng, P. R. McGonigal, A. C. Fahrenbach, M. Frascioni, W. G. Liu, Z. Zhu, Y. Zhao, C. Ke, J. Lei, R. M. Young, S. M. Dyar, D. T. Co, Y. W. Yang, Y. Y. Botros, W. A. Goddard, M. R. Wasielewski, R. D. Astumian, J. F. Stoddart, *J. Am. Chem. Soc.* **2013**, *135*, 18609–18620.
- [18] C. Cheng, P. R. McGonigal, S. T. Schneebeli, H. Li, N. A. Vermeulen, C. Ke, J. F. Stoddart, *Nat. Nanotechnol.* **2015**, *10*, 547–553.
- [19] Y. Jiao, Y. Qiu, L. Zhang, W. G. Liu, H. Mao, H. Chen, Y. Feng, K. Cai, D. Shen, B. Song, X. Y. Chen, X. Li, X. Zhao, R. M. Young, C. L. Stern, M. R. Wasielewski, R. D. Astumian, W. A. Goddard, J. F. Stoddart, *Nature* **2022**, *603*, 265–270.
- [20] C. Pezzato, M. T. Nguyen, D. J. Kim, O. Anamimoghadam, L. Mosca, J. F. Stoddart, *Angew. Chem. Int. Ed.* **2018**, *57*, 9325–9329.
- [21] Y. Qiu, B. Song, C. Pezzato, D. Shen, W. Liu, L. Zhang, Y. Feng, Q. H. Guo, K. Cai, W. Li, H. Chen, M. T. Nguyen, Y. Shi, C. Cheng, R. Dean Astumian, X. Li, J. Fraser Stoddart, *Science* **2020**, *368*, 1247–1253.
- [22] L. Zhang, Y. Qiu, W. G. Liu, H. Chen, D. Shen, B. Song, K. Cai, H. Wu, Y. Jiao, Y. Feng, J. S. W. Seale, C. Pezzato, J. Tian, Y. Tan, X. Y. Chen, Q. H. Guo, C. L. Stern, D. Philp, R. D. Astumian, W. A. Goddard, J. F. Stoddart, *Nature* **2023**, *613*, 280–286.
- [23] L. Ratjen, G. Vantomme, J. M. Lehn, *Chem. Eur. J.* **2015**, *21*, 10070–10081.
- [24] T. Marchetti, L. Gabrielli, D. Frezzato, L. J. Prins, *Angew. Chem. Int. Ed.* **2023**, e202307530.
- [25] G. Vantomme, E. W. Meijer, *Science* **2019**, *363*, 1396–1397.
- [26] S. Rahav, J. Horowitz, C. Jarzynski, *Phys. Rev. Lett.* **2008**, *101*, 140602.
- [27] S. Erbas-Cakmak, S. D. P. Fielden, U. Karaca, D. A. Leigh, C. T. McTernan, D. J. Tetlow, M. R. Wilson, *Science* **2017**, *358*, 340–343.
- [28] D. Del Giudice, S. Di Stefano, *Acc. Chem. Res.* **2023**, *56*, 889–899.
- [29] D. A. Leigh, J. K. Y. Y. Wong, F. Dehez, F. Zerbetto, *Nature* **2003**, *424*, 174–179.
- [30] J. V. Hernández, E. R. Kay, D. A. Leigh, *Science* **2004**, *306*, 1532–1537.
- [31] V. Balzani, M. Clemente-León, A. Credi, B. Ferrer, M. Venturi, A. H. Flood, J. F. Stoddart, *Proc. Natl. Acad. Sci. USA* **2006**, *103*, 1178–1183.
- [32] L. Greb, J.-M. Lehn, *J. Am. Chem. Soc.* **2014**, *136*, 13114–7.
- [33] Z. Wang, P. Erhart, T. Li, Z. Y. Zhang, D. Sampedro, Z. Hu, H. A. Wegner, O. Brummel, J. Libuda, M. B. Nielsen, K. Moth-Poulsen, *Joule* **2021**, *5*, 3116–3136.
- [34] X. Li, S. Cho, J. Wan, G. G. D. Han, *Chem* **2023**, <https://doi.org/10.1016/j.chempr.2023.05.029>.
- [35] M. Ovalle, M. Kathan, R. Toyoda, C. N. Stindt, S. Crespi, B. L. Feringa, *Angew. Chem. Int. Ed.* **2023**, *62*, e202214495.
- [36] S. Shinkai, T. Minami, Y. Kusano, O. Manabe, *J. Am. Chem. Soc.* **1983**, *105*, 1851–1856.
- [37] M. Asakawa, P. R. Ashton, V. Balzani, C. L. Brown, A. Credi, O. A. Matthews, S. P. Newton, F. M. Raymo, A. N. Shipway, N. Spencer, A. Quick, J. F. Stoddart, A. J. P. White, D. J. Williams, *Chem. Eur. J.* **1999**, *5*, 860–875.
- [38] P. Tecilla, D. Bonifazi, *ChemistryOpen* **2020**, *9*, 538–553.
- [39] M. Valentini, F. Fratelloreto, M. Conti, R. Cacciapaglia, D. Del Giudice, S. Di Stefano, *Chem. Eur. J.* **2023**, e202301835.
- [40] R. D. Astumian, *Faraday Discuss.* **2016**, *195*, 583–597.
- [41] E. Penocchio, R. Rao, M. Esposito, *J. Chem. Phys.* **2021**, *155*, 114101.
- [42] A. Sabatino, E. Penocchio, G. Ragazzon, A. Credi, D. Frezzato, *Angew. Chem. Int. Ed.* **2019**, *58*, 14341–14348.
- [43] H. Mauser, G. Gauglitz, *Photokinetics: Theoretical Fundamentals and Applications*, Elsevier, Amsterdam **1998**.
- [44] A. Credi, L. Prodi, *J. Mol. Struct.* **2014**, *1077*, 30–39.
- [45] G. Ragazzon, L. J. Prins, *Nat. Nanotechnol.* **2018**, *13*, 882–889.
- [46] R. D. Astumian, *Chem. Sci.* **2017**, *8*, 840–845.
- [47] C. Pezzato, C. Cheng, J. F. Stoddart, R. D. Astumian, *Chem. Soc. Rev.* **2017**, *46*, 5491–5507.
- [48] R. D. Astumian, *Nat. Commun.* **2019**, *10*, 3837.
- [49] G. Ragazzon, M. Malferrari, A. Arduini, A. Secchi, S. Rapino, S. Silvi, A. Credi, *Angew. Chem. Int. Ed.* **2023**, *62*, e202214265.
- [50] J. J. Grimaldi, J.-M. Lehn, *J. Am. Chem. Soc.* **1979**, *101*, 1333–1334.

- [51] T. Saji, I. Kinoshita, *J. Chem. Soc. Chem. Commun.* **1986**, 716–717.
- [52] S. Selmani, E. Schwartz, J. T. Mulvey, H. Wei, A. Grosvirt-Dramen, W. Gibson, A. I. Hochbaum, J. P. Patterson, R. Ragan, Z. Guan, *J. Am. Chem. Soc.* **2022**, *144*, 7844–7851.
- [53] T. L. Hill, *Free Energy Transduction and Biochemical Cycle Kinetics*, Springer, New York **1989**.
- [54] S. Amano, S. D. P. Fielden, D. A. Leigh, *Nature* **2021**, *594*, 529–534.
- [55] G. De Bo, G. Dolphijn, C. T. McTernan, D. A. Leigh, *J. Am. Chem. Soc.* **2017**, *139*, 8455–8457.
- [56] C. Tian, S. D. P. Fielden, G. F. S. Whitehead, I. J. Vitorica-Yrezabal, D. A. Leigh, *Nat. Commun.* **2020**, *11*, 744.
- [57] S. Borsley, D. A. Leigh, B. M. W. Roberts, *J. Am. Chem. Soc.* **2021**, *143*, 4414–4420.
- [58] M. C. T. Fyfe, P. T. Glink, S. Menzer, J. F. Stoddart, A. J. P. White, D. J. Williams, *Angew. Chem. Int. Ed. Engl.* **1997**, *36*, 2068–2070.
- [59] M. Tena-Solsona, B. Rieß, R. K. Grötsch, F. C. Löhner, C. Wanzke, B. Käsdorf, A. R. Bausch, P. Müller-Buschbaum, O. Lieleg, J. Boekhoven, *Nat. Commun.* **2017**, *8*, 15895.
- [60] L. S. Kariyawasam, C. S. Hartley, *J. Am. Chem. Soc.* **2017**, *139*, 11949–11955.
- [61] B. Rieß, R. K. Grötsch, J. Boekhoven, *Chem* **2020**, *6*, 552–578.
- [62] F. Schnitter, A. M. Bergmann, B. Winkeljann, J. Rondon Fores, O. Lieleg, J. Boekhoven, *Nat. Protoc.* **2021**, *16*, 3901–3932.
- [63] X. Chen, M. A. Würbser, J. Boekhoven, *Acc. Mater. Res.* **2023**, *4*, 416–426.
- [64] L. S. Kariyawasam, M. M. Hossain, C. S. Hartley, *Angew. Chem. Int. Ed.* **2021**, *60*, 12648–12658.
- [65] S. Borsley, E. Kreidt, D. A. Leigh, B. M. W. Roberts, *Nature* **2022**, *604*, 80–85.
- [66] M. Fialkowski, K. J. M. Bishop, R. Klajn, S. K. Smoukov, C. J. Campbell, B. a Grzybowski, *J. Phys. Chem. B* **2006**, *110*, 2482–96.
- [67] E. Mattia, S. Otto, *Nat. Nanotechnol.* **2015**, *10*, 111–119.
- [68] G. Ashkenasy, T. M. Hermans, S. Otto, A. F. Taylor, *Chem. Soc. Rev.* **2017**, *46*, 2543–2554.
- [69] M. R. Wilson, J. Solà, A. Carlone, S. M. Goldup, N. Lebrasseur, D. A. Leigh, *Nature* **2016**, *534*, 235–240.
- [70] E. Liu, S. Cherraben, L. Boulo, C. Troufflard, B. Hasenknopf, G. Vives, M. Sollogoub, *Chem* **2023**, *9*, 1147–1163.
- [71] D. G. Blackmond, *Angew. Chem. Int. Ed.* **2009**, *48*, 2648–2654.
- [72] S. Amano, M. Esposito, E. Kreidt, D. A. Leigh, E. Penocchio, B. M. W. Roberts, *J. Am. Chem. Soc.* **2022**, *144*, 20153–20164.
- [73] M. Alvarez-Pérez, S. M. Goldup, D. A. Leigh, A. M. Z. Slawin, *J. Am. Chem. Soc.* **2008**, *130*, 1836–1838.
- [74] S. Kozuch, S. Shaik, *J. Am. Chem. Soc.* **2006**, *128*, 3355–3365.
- [75] S. Kozuch, S. Shaik, *Acc. Chem. Res.* **2011**, *44*, 101–110.
- [76] E. Penocchio, G. Ragazzon, *Small* **2023**, *19*, 2206188.
- [77] S. Borsley, D. A. Leigh, B. M. W. Roberts, I. J. Vitorica-Yrezabal, *J. Am. Chem. Soc.* **2022**, *144*, 17241–17248.
- [78] V. Serreli, C.-F. Lee, E. R. Kay, D. A. Leigh, *Nature* **2007**, *445*, 523–527.
- [79] N. Tamaoki, M. Wada, *J. Am. Chem. Soc.* **2006**, *128*, 6284–6285.
- [80] P. K. Hashim, R. Thomas, N. Tamaoki, *Chem. Eur. J.* **2011**, *17*, 7304–7312.
- [81] N. P. M. Huck, W. F. Jager, B. De Lange, B. L. Feringa, *Science* **1996**, *273*, 1686–1688.
- [82] R. Göstl, S. Hecht, *Angew. Chem. Int. Ed.* **2014**, *53*, 8784–8787.
- [83] R. Göstl, S. Hecht, *Chem. Eur. J.* **2015**, *21*, 4422–4427.
- [84] M. Kathan, F. Eisenreich, C. Jurissek, A. Dallmann, J. Gurke, S. Hecht, *Nat. Chem.* **2018**, *10*, 1031–1036.
- [85] J. W. Freedy, A. Méndez-Ardoy, S. Kwangmettadam, D. Bochicchio, B. Matt, M. C. A. Stuart, J. Huskens, N. Katsonis, G. M. Pavan, T. Kudernac, *Proc. Natl. Acad. Sci. USA* **2017**, *114*, 11850–11855.
- [86] P. J. M. Van Haastert, P. N. Devreotes, *Nat. Rev. Mol. Cell Biol.* **2004**, *5*, 626–634.
- [87] M. Feng, M. K. Gilson, *Annu. Rev. Biophys.* **2020**, *49*, 87–105.
- [88] N. S. Mandal, A. Sen, R. D. Astumian, *J. Am. Chem. Soc.* **2023**, *145*, 5730–5738.
- [89] G. Ragazzon, M. Baroncini, S. Silvi, M. Venturi, A. Credi, *Nat. Nanotechnol.* **2015**, *10*, 70–75.
- [90] S. J. Wezenberg, *Chem. Lett.* **2020**, *49*, 609–615.
- [91] A. D. W. Kennedy, R. G. DiNardi, L. L. Fillbrook, W. A. Donald, J. E. Beves, *Chem. Eur. J.* **2022**, *28*, e202104461.
- [92] J. Gemen, J. R. Church, T.-P. Ruoko, N. Durandin, M. J. Bialek, M. Weissenfels, M. Feller, M. Kazes, V. A. Borin, M. Odaybat, R. Kalepu, Y. Diskin-Posner, D. Oron, M. J. Fuchter, A. Primagi, I. Schapiro, R. Klajn, *ChemRxiv preprint* **2023**, <https://doi.org/10.26434/chemrxiv-2023-gq2-h0>.
- [93] E. M. Geertsema, S. J. van der Molen, M. Martens, B. L. Feringa, *Proc. Natl. Acad. Sci. USA* **2009**, *106*, 16919–16924.
- [94] B. L. Feringa, *Angew. Chem. Int. Ed.* **2017**, *56*, 11060–11078.
- [95] S. J. Wezenberg, B. L. Feringa, *Nat. Commun.* **2018**, *9*, 1984.
- [96] P. Štacko, J. C. M. Kistemaker, T. Van Leeuwen, M. Chang, E. Otten, B. L. Feringa, *Science* **2017**, *356*, 964–968.
- [97] Q. Li, G. Fuks, E. Moulin, M. Maaloum, M. Rawiso, I. Kulic, J. T. Foy, N. Giuseppone, *Nat. Nanotechnol.* **2015**, *10*, 161–165.
- [98] J. T. Foy, Q. Li, A. Goujon, J. R. Colard-Itté, G. Fuks, E. Moulin, O. Schiffmann, D. Dattler, D. P. Funeriu, N. Giuseppone, *Nat. Nanotechnol.* **2017**, *12*, 540–545.
- [99] C. Gao, A. Vargass Jentzsch, E. Moulin, N. Giuseppone, *J. Am. Chem. Soc.* **2022**, *144*, 9845–9852.
- [100] M. Kathan, S. Crespi, N. O. Thiel, D. L. Stares, D. Morsa, J. de Boer, G. Pacella, T. van den Enk, P. Kobauri, G. Portale, C. A. Schalley, B. L. Feringa, *Nat. Nanotechnol.* **2022**, *17*, 159–165.
- [101] R. Eelkema, M. M. Pollard, J. Vicario, N. Katsonis, B. S. Ramon, C. W. M. Bastiaansen, D. J. Broer, B. L. Feringa, *Nature* **2006**, *440*, 163.
- [102] A. Gerwien, F. Gnannt, P. Mayer, H. Dube, *Nat. Chem.* **2022**, *14*, 670–676.
- [103] R. Chen, S. Neri, L. J. Prins, *Nat. Nanotechnol.* **2020**, *15*, 868–874.
- [104] S. A. P. Van Rossum, M. Tena-Solsona, J. H. Van Esch, R. Eelkema, J. Boekhoven, *Chem. Soc. Rev.* **2017**, *46*, 5519–5535.
- [105] S. Borsley, D. A. Leigh, B. M. W. Roberts, *Nat. Chem.* **2022**, *14*, 728–738.
- [106] N. Singh, G. J. M. Formon, S. De Piccoli, T. M. Hermans, *Adv. Mater.* **2020**, *32*, 1906834.
- [107] S. De, R. Klajn, *Adv. Mater.* **2018**, *30*, 1706750.
- [108] J. Leira-Iglesias, A. Tassoni, T. Adachi, M. Stich, T. M. Hermans, *Nat. Nanotechnol.* **2018**, *13*, 1021–1028.
- [109] I. Maity, N. Wagner, R. Mukherjee, D. Dev, E. Peacock-Lopez, R. Cohen-Luria, G. Ashkenasy, *Nat. Commun.* **2019**, *10*, 4636.
- [110] F. Schnitter, B. Rieß, C. Jandl, J. Boekhoven, *Nat. Commun.* **2022**, *13*, 2816.
- [111] M. G. Howlett, A. H. J. Engwerda, R. J. H. Scanes, S. P. Fletcher, *Nat. Chem.* **2022**, *14*, 805–810.
- [112] I. R. Epstein, J. A. Pojman, *An Introduction to Nonlinear Chemical Dynamics*, Oxford University Press, New York **1998**.
- [113] S. Maiti, I. Fortunati, C. Ferrante, P. Scrimin, L. J. Prins, *Nat. Chem.* **2016**, *8*, 725–731.

- [114] B. A. K. Kriebisch, A. Jussupow, A. M. Bergmann, F. Kohler, H. Dietz, V. R. I. Kaila, J. Boekhoven, *J. Am. Chem. Soc.* **2020**, *142*, 20837–20844.
- [115] M. Tena-Solsona, C. Wanzke, B. Riess, A. R. Bausch, J. Boekhoven, *Nat. Commun.* **2018**, *9*, 2044.
- [116] P. Solís Muñana, G. Ragazzon, J. Dupont, C. Z. J. Ren, L. J. Prins, J. L. Y. Chen, *Angew. Chem. Int. Ed.* **2018**, *57*, 16469–16474.
- [117] S. Bal, K. Das, S. Ahmed, D. Das, *Angew. Chem. Int. Ed.* **2019**, *58*, 244–247.
- [118] P. S. Schwarz, M. Tena-Solsona, K. Dai, J. Boekhoven, *Chem. Commun.* **2022**, 58, 1284–1297.
- [119] E. Penocchio, R. Rao, M. Esposito, *Nat. Commun.* **2019**, *10*, 3865.
- [120] K. Das, L. Gabrielli, L. J. Prins, *Angew. Chem. Int. Ed.* **2021**, *60*, 20120–20143.
- [121] A. Sorrenti, J. Leira-Iglesias, A. Sato, T. M. Hermans, *Nat. Commun.* **2017**, *8*, 15899.
- [122] A. M. Bergmann, J. Bauermann, G. Bartolucci, C. Donau, M. Stasi, A.-L. Holtmannspötter, F. Jülicher, C. A. Weber, J. Boekhoven, *bioRxiv preprint* **2023**, <https://doi.org/10.1101/2023.01.31.526480>.
- [123] T. Schnitzer, M. D. Preuss, J. van Basten, S. M. C. Schoenmakers, A. J. H. Spiering, G. Vantomme, E. W. Meijer, *Angew. Chem. Int. Ed.* **2022**, *61*, e202206738.
- [124] D. Del Giudice, E. Spatola, M. Valentini, G. Ercolani, S. Di Stefano, *ChemSystemsChem* **2022**, *4*, e202200023.
- [125] H. Fanlo-Virgós, A.-N. R. Alba, S. Hamieh, M. Colomb-Delsuc, S. Otto, *Angew. Chem. Int. Ed.* **2014**, *53*, 11346–11350.
- [126] F. Avanzini, E. Penocchio, G. Falasco, M. Esposito, *J. Chem. Phys.* **2021**, *154*, 094114.
- [127] S. Corra, M. T. Bakic, J. Groppi, M. Baroncini, S. Silvi, E. Penocchio, M. Esposito, A. Credi, *Nat. Nanotechnol.* **2022**, *17*, 746–751.
- [128] L. Binks, S. Borsley, T. R. Gingrich, D. A. Leigh, E. Penocchio, B. M. W. Roberts, *Chem* **2023**, <https://doi.org/10.1016/j.chempr.2023.05.035>.
- [129] S. Di Noja, M. Garrido, L. Gualandi, G. Ragazzon, *Chem. Eur. J.* **2023**, *29*, e202300295.
- [130] J. Ehrich, D. A. Sivak, *Front. Phys.* **2023**, *11*, 1108357.
- [131] S. Amano, M. Esposito, E. Kreidt, D. A. Leigh, E. Penocchio, B. M. W. Roberts, *Nat. Chem.* **2022**, *14*, 530–537.
- [132] E. Penocchio, F. Avanzini, M. Esposito, *J. Chem. Phys.* **2022**, *157*, 034110.
- [133] H. Wackerhage, U. Hoffmann, D. Essfeld, D. Leyk, K. Mueller, J. Zange, *J. Appl. Physiol.* **1998**, *85*, 2140–2145.
- [134] D. Kondepudi, I. Prigogine, *Modern Thermodynamics: From Heat Engines to Dissipative Structures*, Wiley, Hoboken **2015**.
- [135] M. Bilancioni, M. Esposito, E. Penocchio, *J. Chem. Phys.* **2023**, *158*, 224104.
- [136] G. Falasco, T. Cossetto, E. Penocchio, M. Esposito, *New J. Phys.* **2019**, *21*, 073005.
- [137] G. Falasco, R. Rao, M. Esposito, *Phys. Rev. Lett.* **2018**, *121*, 108301.
- [138] I. R. Epstein, B. Xu, *Nat. Nanotechnol.* **2016**, *11*, 312–319.
- [139] A. Ianeselli, A. Salditt, C. Mast, B. Ercolano, C. L. Kufner, B. Scheu, D. Braun, *Nat. Rev. Phys.* **2023**, *5*, 185–195.
- [140] D. M. Busiello, S. Liang, F. Piazza, P. De Los Rios, *Commun. Chem.* **2021**, *4*, 16.
- [141] C. Bonfio, C. Caumes, C. D. Duffy, B. H. Patel, C. Percivalle, M. Tsanakopoulou, J. D. Sutherland, *J. Am. Chem. Soc.* **2019**, *141*, 3934–3939.
- [142] M. Kaufmann, *Int. J. Mol. Sci.* **2009**, *10*, 1853–1871.
- [143] D. Deamer, A. L. Weber, *Cold Spring Harbor Perspect. Biol.* **2010**, *2*, a004929.
- [144] L. Boiteau, R. Pascal, *Origins Life Evol. Biospheres* **2011**, *41*, 23–33.
- [145] K. B. Muchowska, S. J. Varma, J. Moran, *Chem. Rev.* **2020**, *120*, 7708–7744.
- [146] E. Smith, H. J. Morowitz, *Proc. Natl. Acad. Sci. USA* **2004**, *101*, 13168–13173.
- [147] M. Aleksandrova, C. Bonfio, *EMBO Rep.* **2022**, *23*, e55679.
- [148] C. Bonfio, E. Godino, M. Corsini, F. Fabrizi de Biani, G. Guella, S. S. Mansy, *Nat. Catal.* **2018**, *1*, 616–623.
- [149] A. Wachtel, R. Rao, M. Esposito, *J. Chem. Phys.* **2022**, *157*, 024109.
- [150] K. Schmidt-Rohr, *ACS Omega* **2020**, *5*, 2221–2233.
- [151] C. T. Walsh, B. P. Tu, Y. Tang, *Chem. Rev.* **2018**, *118*, 1460–1494.
- [152] W. Nitschke, B. Schoepp-Cothenet, S. Duval, K. Zuchan, O. Farr, F. Baymann, F. Panico, A. Minguzzi, E. Branscomb, M. J. Russell, *Electrochem. Sci. Adv.* **2023**, *3*, e2100192.
- [153] H. Hess, J. L. Ross, *Chem. Soc. Rev.* **2017**, *46*, 5570–5587.
- [154] S. Pigolotti, P. Sartori, *J. Stat. Phys.* **2016**, *162*, 1167–1182.
- [155] T. Göppel, B. Obermayer, I. A. Chen, U. Gerland, *bioRxiv preprint* **2021**, <https://doi.org/10.1101/2021.08.06.455386>.
- [156] A. Mariani, J. D. Sutherland, *Angew. Chem. Int. Ed.* **2017**, *56*, 6563–6566.
- [157] T. H. Wright, C. Giurgiu, W. Zhang, A. Radakovic, D. K. O'Flaherty, L. Zhou, J. W. Szostak, *J. Am. Chem. Soc.* **2019**, *141*, 18104–18112.
- [158] J. J. Hopfield, *Proc. Natl. Acad. Sci. USA* **1974**, *71*, 4135–4139.
- [159] H. Aoyanagi, S. Pigolotti, S. Ono, S. Toyabe, *Biophys. J.* **2023**, *122*, 1334–1341.
- [160] V. Galstyan, K. Husain, F. Xiao, A. Murugan, R. Phillips, *eLife* **2020**, *9*, e60415.
- [161] A. Coskun, M. Banaszak, R. D. Astumian, J. F. Stoddart, B. a Grzybowski, *Chem. Soc. Rev.* **2012**, *41*, 19–30.
- [162] E. Moulin, L. Faour, C. C. Carmona-vargas, N. Giuseppone, *Adv. Mater.* **2019**, *31*, 1906036.
- [163] L. Feng, Y. Qiu, Q.-H. Guo, Z. Chen, J. S. W. Seale, K. He, H. Wu, Y. Feng, O. K. Farha, R. D. Astumian, J. F. Stoddart, *Science* **2021**, *374*, 1215–1221.
- [164] D. Thomas, D. J. Tetlow, Y. Ren, S. Kassem, U. Karaca, D. A. Leigh, *Nat. Nanotechnol.* **2022**, *17*, 701–707.
- [165] A. Walther, *Adv. Mater.* **2019**, *31*, 1905111.
- [166] C. Kaspar, B. J. Ravoo, W. G. van der Wiel, S. V. Wegner, W. H. P. Pernice, *Nature* **2021**, *594*, 345–355.
- [167] C. Van Den Broeck, R. Kawai, *Phys. Rev. Lett.* **2006**, *96*, 210601.
- [168] Y. Ren, R. Jamagne, D. J. Tetlow, D. A. Leigh, *Nature* **2022**, *612*, 78–82.
- [169] W. M. Haynes, *CRC Handbook of Chemistry and Physics*, CRC, Boca Raton **2014**.
- [170] H. Zhou, T. Yamada, N. Kimizuka, *J. Am. Chem. Soc.* **2016**, *138*, 10502–10507.
- [171] H. Arazoe, D. Miyajima, K. Akaike, F. Araoka, E. Sato, T. Hikima, M. Kawamoto, T. Aida, *Nat. Mater.* **2016**, *15*, 1084–1089.
- [172] G. Mahmud, C. J. Campbell, K. J. M. Bishop, Y. A. Komarova, O. Chaga, S. Soh, S. Huda, K. Kandere-Grzybowska, B. A. Grzybowski, *Nat. Phys.* **2009**, *5*, 606–612.
- [173] A. H. Gelebart, D. Jan Mulder, M. Varga, A. Konya, G. Vantomme, E. W. Meijer, R. L. B. Selinger, D. J. Broer, *Nature* **2017**, *546*, 632–636.
- [174] F. Lancia, A. Ryabchun, N. Katsonis, *Nat. Chem. Rev.* **2019**, *3*, 536–551.
- [175] S. Iamsaard, S. J. Aßhoff, B. Matt, T. Kudernac, J. J. L. M. Cornelissen, S. P. Fletcher, N. Katsonis, *Nat. Chem.* **2014**, *6*, 229–235.
- [176] J. Hou, A. Mondal, G. Long, L. de Haan, W. Zhao, G. Zhou, D. Liu, D. J. Broer, J. Chen, B. L. Feringa, *Angew. Chem. Int. Ed.* **2021**, *60*, 8251–8257.

- [177] H. Zhang, H. Zeng, A. Eklund, H. Guo, A. Priimagi, O. Ikkala, *Nat. Nanotechnol.* **2022**, *17*, 1303–1310.
- [178] M. Shetty, A. Walton, S. R. Gathmann, M. A. Ardagh, J. Gopeesingh, J. Resasco, T. Birol, Q. Zhang, M. Tsapatsis, D. G. Vlachos, P. Christopher, C. D. Frisbie, O. A. Abdelrahman, P. J. Dauenhauer, *ACS Catal.* **2020**, *10*, 12666–12695.
- [179] G. R. Wittreich, S. Liu, P. J. Dauenhauer, D. G. Vlachos, *Sci. Adv.* **2022**, *8*, eabl6576.
- [180] B. Lau, O. Kedem, M. Kodaimati, M. A. Ratner, E. A. Weiss, *Adv. Energy Mater.* **2017**, *7*, 1701000.
- [181] R. R. Adžić, K. I. Popov, M. A. Pamić, *Electrochim. Acta* **1978**, *23*, 1191–1196.
- [182] F. Sordello, F. Pellegrino, M. Prozzi, C. Minero, V. Maurino, *ACS Catal.* **2021**, *11*, 6484–6488.
- [183] Y. Hioki, M. Costantini, J. Griffin, K. C. Harper, M. P. Merini, B. Nissl, Y. Kawamata, P. S. Baran, *Science* **2023**, *380*, 81–87.
- [184] G. Haran, I. Riven, *J. Phys. Chem. B* **2023**, *127*, 4687–4693.
- [185] M. Corbella, G. P. Pinto, S. C. L. Kamerlin, *Nat. Chem. Rev.* **2023**, *7*, 536–547.
- [186] G. Hu, J. A. Pojman, S. K. Scott, M. M. Wrobel, A. F. Taylor, *J. Phys. Chem. B* **2010**, *114*, 14059–14063.
- [187] A. Sharko, D. Livitz, S. De Piccoli, K. J. M. Bishop, T. M. Hermans, *Chem. Rev.* **2022**, *122*, 11759–11777.
- [188] B. Borderie, D. Lavabre, J. C. Micheau, J. P. Laplante, *J. Phys. Chem.* **1992**, *96*, 2953–2961.
- [189] S. Amano, S. Borsley, D. A. Leigh, Z. Sun, *Nat. Nanotechnol.* **2021**, *16*, 1057–1067.
- [190] G. M. Whitesides, R. F. Ismagilov, *Science* **1999**, *284*, 89–92.
- [191] P. Van Duppen, E. Daines, W. E. Robinson, W. T. S. Huck, *J. Am. Chem. Soc.* **2023**, *145*, 7559–7568.
- [192] N. A. Yewdall, A. F. Mason, J. C. M. van Hest, *Interface Focus* **2018**, *8*, 20180023.
- [193] I. Aprahamian, S. M. Goldup, *J. Am. Chem. Soc.* **2023**, *145*, 14169–14183.

Manuscript received: July 4, 2023

Accepted manuscript online: August 6, 2023

Version of record online: August 25, 2023